



GRADUATE SCHOOL  
EAST TENNESSEE STATE UNIVERSITY

East Tennessee State University  
Digital Commons @ East  
Tennessee State University

---

Electronic Theses and Dissertations

Student Works


---

8-2023

## Mapping The Binding Site Within Integrin $\alpha$ D $\beta$ 2 for Carboxyethylpyrrole (CEP)-Modified Proteins

Afia Prema  
East Tennessee State University

Follow this and additional works at: <https://dc.etsu.edu/etd>

 Part of the [Biology Commons](#)

---

### Recommended Citation

Prema, Afia, "Mapping The Binding Site Within Integrin  $\alpha$ D $\beta$ 2 for Carboxyethylpyrrole (CEP)-Modified Proteins" (2023). *Electronic Theses and Dissertations*. Paper 4232. <https://dc.etsu.edu/etd/4232>

This Thesis - embargo is brought to you for free and open access by the Student Works at Digital Commons @ East Tennessee State University. It has been accepted for inclusion in Electronic Theses and Dissertations by an authorized administrator of Digital Commons @ East Tennessee State University. For more information, please contact [digilib@etsu.edu](mailto:digilib@etsu.edu).

Mapping The Binding Site Within Integrin  $\alpha_D\beta_2$   
for Carboxyethylpyrrole (CEP)-Modified Proteins

---

A thesis  
presented to  
the faculty of the Department of Biological Sciences  
East Tennessee State University

In partial fulfillment  
of the requirements for the degree  
Master of Science in Biological Sciences

---

by  
Afia Maheda Prema  
August 2023

---

Dr. Valentin Yakubenko, Chair

Dr. Dhirendra Kumar

Dr. Patrick Bradshaw

Keywords: chronic inflammation, macrophage, integrins, CEP-modified protein,  
mutagenesis, protein-protein binding

## ABSTRACT

### Mapping The Binding Site Within Integrin $\alpha_D\beta_2$ for Carboxyethylpyrrole (CEP)-Modified Proteins

by

Afia Maheda Prema

Neutrophils and macrophages accumulate at sites of inflammation and cause chronic inflammation leading to various diseases. Therefore, to better understand chronic disease pathways it is important to investigate the properties of macrophage accumulation in inflamed tissues. The I-domain of the macrophage receptor integrin  $\alpha_D\beta_2$  plays a vital role in macrophage retention by binding to CEP (carboxyethyl pyrrole), a ligand available at inflammatory sites. This thesis mainly focuses on evaluating the binding site within integrin  $\alpha_D\beta_2$  that binds carboxyethyl pyrrole (CEP)-modified proteins. So, a recombinant plasmid construct containing the integrin I-domain was developed. Seven non-conserved amino acids were mutated by PCR-site-directed mutagenesis to create a mutant construct. After expressing in *E. coli*, the binding affinities of wild-type and mutant I-domains to CEP were analyzed using biolayer interferometry. It was found that a patch of seven positively charged amino acids contributes to the strong binding of the I domain to CEP.

Copyright 2023 by Afia Maheda Prema

All Rights Reserved

## ACKNOWLEDGMENTS

I am thankful to my committee chair and mentor Dr. Valentin Yakubenko for providing me with the opportunity to work in his lab and for his unconditional support and motivation. Under his supervision, I successfully and efficiently completed my thesis work. It was quite a learning experience. My lab mates also helped me greatly. Moreover, I also express my gratitude to my committee members Dr. Patrick Bradshaw and Dr. Dhirendra Kumar for their valuable comments and guidance which helped me to be disciplined and goal oriented. I am especially grateful for my parents who always encouraged and believed in me. Without their support, this experience would not have been possible. I am also grateful for the encouragement and support from my friends.

## TABLE OF CONTENTS

ABSTRACT.....	2
ACKNOWLEDGMENTS .....	4
LIST OF TABLES .....	8
LIST OF FIGURES .....	9
CHAPTER 1. INTRODUCTION .....	11
The Initiation of Inflammation.....	12
Acute Inflammatory Response.....	12
First Wave of Inflammation: Neutrophil Recruitment.....	13
Second Wave of Inflammation: Macrophage Migration .....	14
Macrophage Phenotypes and Inflammation Resolution .....	14
Chronic Inflammation.....	16
Correlation Between Chronic Inflammation and Macrophage Accumulation .....	17
The Integrin Family .....	18
Structure.....	18
The Structure of Integrin Subunits.....	19
Integrin $\beta_2$ .....	21
Integrin $\alpha_D\beta_2$ .....	23
CEP- Integrin $\alpha_D\beta_2$ -Mediated Inflammation.....	24
CHAPTER 2. MATERIAL AND EXPERIMENTAL PROCEDURES .....	26
Materials .....	26
Experimental Procedure.....	26

Identification of Amino Acids for Mutation .....	26
Protein BLAST and 3D Protein Structure Prediction. ....	26
Introduction of the Mutations .....	26
Recombinant Plasmid Generation.....	26
Generation of Mutagenic Primers.....	28
PCR Site-Directed Mutagenesis. ....	28
XL1-B Transformation. ....	30
Recombinant Plasmid DNA Isolation.....	30
Protein Expression .....	31
BL21 Transformation.....	31
Cell Culture.....	32
Protein Expression with IPTG. ....	32
Protein Isolation .....	32
Bacterial Cell Lysis.....	32
Ni-NTA Column Chromatography.....	33
Protein Dialysis.....	33
Protein Analysis .....	34
SDS-PAGE. ....	34
BCA Assay.....	34
Biolayer Interferometry .....	35
Amine Reactive (ARG2) Biosensor Assays. ....	35

Experimental Design Flow Through.....	36
CHAPTER 3. RESULTS.....	37
Selection of $\alpha_D$ I-Domain Amino Acids Important for Binding to CEP.....	37
Recombinant Plasmid Generation.....	40
Verification of the Presence of the $\alpha_D$ I-Domain in the pET28a Vector.....	41
Primer Design and Mutant Construct Generation.....	42
First Mutation Generation.....	43
Second Mutation Generation.....	45
Third Mutation Generation (RK to GA).....	46
The Final Sequence of the Mutated $\alpha_D$ I-Domain.....	48
Protein Purification and Analysis.....	48
The $\alpha_D$ I-domain Mutant Demonstrated a Reduction in Binding to CEP Compared to the Wild-Type $\alpha_D$ I-Domain.....	49
CHAPTER 4. DISCUSSION.....	51
REFERENCES.....	54
VITA.....	59



## LIST OF TABLES

Table 1. Digestion reaction component with respective quantity .....	27
Table 2. Ligation reaction component with respective quantity .....	28
Table 3. PCR sample reaction components for mutagenesis .....	29
Table 4. QuikChange II site-directed mutagenesis cycling conditions.....	29
Table 5. Selection process of $\alpha$ D I-domain amino acids for mutagenesis .....	38
Table 6. Mutagenic construct generation using the newly designed primers .....	43

## LIST OF FIGURES

Figure 1. Macrophage polarization.....	15
Figure 2. The acute inflammatory response to a bacterial infection.....	16
Figure 3. Chronic inflammation.....	17
Figure 4. The integrin family consists of $\alpha$ and $\beta$ -subunits. ....	19
Figure 5. Representation of a prototypical $\alpha$ I-domain-containing integrin heterodimer.....	20
Figure 6. Structure of integrin.....	21
Figure 7. Bi-directional activation of integrins during leukocyte-endothelial cell interaction.....	22
Figure 8. The leukocyte adhesion cascade and its regulation by integrins.....	23
Figure 9. Generation of CEP and EP. ....	24
Figure 10. NCBI BLAST analysis and structure prediction of the integrin $\alpha$ D I-domain. ....	37
Figure 11. Prediction using SWISS model of the $\alpha$ D I-domain structure before and after mutation. ....	39
Figure 12. The pET-28a(+) vector.....	40
Figure 13. Verification of the presence of the $\alpha$ D I-domain in pET28a using a single restriction enzyme. ....	41
Figure 14. Verification of the presence of the $\alpha$ D I-domain in pET28a using PCR of the insert .....	42
Figure 15. DNA gel electrophoresis of isolated mutant DNA after the first PCR site-directed mutagenesis.....	44
Figure 16. The first DNA mutation was confirmed using Oligo Software.....	44
Figure 17. DNA gel electrophoresis of isolated mutant DNA after the second PCR site- directed mutagenesis. ....	45
Figure 18. Confirmation of the success of the second DNA mutagenesis experiment.....	46

Figure 19. DNA gel electrophoresis of isolated mutant DNA after the third PCR site-directed mutagenesis experiment. ....	47
Figure 20. The third and final DNA mutagenesis step was confirmed.....	47
Figure 21. SDS-polyacrylamide gel electrophoresis (12%) for isolated WT and mutant $\alpha$ D I-domain proteins. ....	49
Figure 22. WT and mutant $\alpha$ D I-domain binding to CEP. ....	50

## CHAPTER 1. INTRODUCTION

Inflammation is considered to be an important mechanism through which the human body regulates health and disease. Inflammation is induced when the host is exposed to a pathogen or injury thereby initiating a protective defense or healing response (Freire and Van Dyke 2013). Inflammation includes a chain of reactions leading to the repair of the damaged tissues. These reactions are important host responses such as the elevated permeability of micro-vessels to allow the migration of several types of immune cells to the site of injury and increased rates of apoptosis (Schmid-Schönbein 2006).

However, if the inflammatory process continues unchecked for long periods, it becomes chronic inflammation possibly predisposing to disease. In response to pathogens, damaged cells, or toxic compounds, dysregulated inflammation is initiated in different organs such as the heart, reproductive system, liver, kidney, lungs, and brain resulting in various adverse health conditions. It has been found that the reactions of the inflammatory cascade are common in the pathogenesis of chronic diseases such as heart disease, diabetes, cancer, arthritis, and many others (Chen et al. 2017; Meizlish et al. 2021). Therefore, it is important to find the molecular basis of this chronic inflammatory dysregulation for the discovery of new targets and treatments against the associated complications.

Innate immune cells such as macrophages play a vital role in both acute and chronic inflammatory processes. In the late 19<sup>th</sup> century, Metchnikoff first identified macrophages (Ponzoni et al. 2018). Macrophages work as a link between the innate and adaptive immune systems. Macrophages possess innate plasticity to alter their phenotype and show a tendency to migrate to sites of inflammation making them good candidates for new treatments to target various chronic diseases (Davignon et al. 2013). The goal of my research was to identify a specific site within macrophage integrin  $\alpha_D\beta_2$  that binds CEP-modified proteins. CEP-modified proteins work as ligands for  $\alpha_D\beta_2$  and  $\alpha_M\beta_2$  integrins.

### *The Initiation of Inflammation*

An inflammatory response is first initiated by the innate immune system consisting of macrophages, dendritic cells, or neutrophils. These innate immune cells express pattern recognition receptors (PRRs) on their surface that bind to different damaged tissues containing pathogen-associated molecular patterns (PAMPs) or damage-associated molecular patterns (DAMP) on damaged tissues. These binding events facilitate the secretion of inflammatory cytokines such as IL-1 $\beta$ , IL-6, and TNF- $\alpha$ , and many different chemokines (Williams et al. 2011). These inflammatory mediators can modulate the leukocyte adhesion and transmigration through the endothelium at the injury site. These infiltrated leukocytes are responsible for mediating oxidative stress in the tissue (Ou et al. 2021a). Such oxidative stress modifies the extracellular matrix (ECM) in inflamed tissues yielding protein lysine modifications (Yakubenko et al. 2018a)

### *Acute Inflammatory Response*

Acute inflammation occurs in response to trauma or injury. The main goal for acute inflammation is to abate the inflammation and return the tissue to equilibrium (Chow et al. 2005). During acute inflammation, different endogenous anti-inflammatory cytokines are released to eradicate the initial inflammation. Different innate immune cells such as macrophages and dendritic cells become active at this stage. Arrival of microorganisms can be sensed by germline-encoded pattern recognition receptors (PRRs). These sensors can identify pathogen-associated molecular pattern (PAMPs), which are conserved among microbial species. PRRs can also recognize damage associated molecular patterns (DAMPs), which are released by damaged cells of the host. During acute inflammation, proinflammatory cytokines such as tumor necrosis factor (TNF), IL-6 and IL-1 work together to make an inhospitable environment for the pathogen (Takeuchi and Akira 2010). This cytokine storm can activate more immune cells to defend against pathogens. However, the response to the

acute inflammation is dependent on the environment and the age of the host (Kumar et al. 2004). During acute inflammation three types of events mainly take place. These are a) increased blood supply to the inflamed tissue, b) capillary permeability changes, and c) leukocyte migration to the site of inflammation (Rankin 2004). Through these events, inflammatory infiltrates mainly aim to fight the pathogens and repair tissue damage. However, sometimes uncontrolled migration of leukocytes can result in 'by-stander' tissue injury and organ dysfunction (Sugimoto et al. 2019) .

#### *First Wave of Inflammation: Neutrophil Recruitment*

In response to pathogens, tissue injury, or infection the very first responders are neutrophils. They have high microbicidal activity with a short lifespan and can migrate throughout the circulation as needed. Neutrophils possess the heterogeneity and plasticity to differentiate into discrete subsets. Neutrophils are generally non-resident immune cells because they are generated within bone marrow with the capability of entering the circulation quickly when needed (Pradeep Kumar et al. 2018). The host defense mechanism at the injury site is executed through a tightly regulated adhesive cascade and migration process. Inflammation-mediated cytokine secretion increases the levels of specific plasma membrane receptors on neutrophils, which ultimately helps the neutrophils penetrate the endothelium (Voisin and Nourshargh 2013). Being the first wave of the immune response, neutrophils secrete peroxidases at the site of injury, which leads to oxidative modifications of macromolecules in the ECM to mark the site (Williams et al. 2011). Neutrophils can also execute phagocytosis, degranulation, or the formation of neutrophil extracellular traps. Neutrophil apoptosis can inhibit chronic disorders. However, irregular or deregulated neutrophil apoptosis can induce chronic diseases like cancer by increasing metastasis (Brostjan and Oehler 2020). So, such uncontrolled neutrophil recruitment brings about several pathologic outcomes which need further investigation.

### *Second Wave of Inflammation: Macrophage Migration*

To induce a rapid host response during acute inflammation neutrophils, generate excessive reactive oxygen species. At the same time different chemokines, cytokines, and many proinflammatory mediators are released thereby attracting more neutrophils as well as adaptive immune cells such as B-cells and T-cells (Ai and Udalova 2020). Chemokine release triggered by neutrophils is capable of controlling leukocyte recruitment and regulating the transition from recruitment of neutrophils to the recruitment of mononuclear leukocytes or monocytes (McLoughlin et al. 2004). It has been found that among the secreted cytokines, IL-6 has the greatest effect in shifting leukocyte recruitment by decreasing neutrophil and facilitating monocyte recruitment (Kaplanski 2003). These circulating monocytes transmigrate to sites of tissue injury by extravasation and differentiate into macrophages. Tissue-resident immune cells, being diverse and highly plastic, have several functions during inflammation including phagocytosis, angiogenesis control and ECM remodeling. They also play roles in maintaining tissue homeostasis, tissue regeneration and tissue development. Unfortunately, continuous insult (through chronic environmental stress, genetic predisposition, or aging) leads to chronic pathological outcomes (Oishi and Manabe 2018).

### *Macrophage Phenotypes and Inflammation Resolution*

In response to different stimuli, macrophage activation occurs. According to the pathogen or injury type phenotypic heterogeneity develops and macrophages polarize. Based on their activation status phenotypically-polarized macrophages can be divided into two groups, activated M1-like and alternatively activated M2-like macrophages (Bashir et al. 2016). Activated M1 macrophages can trigger pro-inflammatory cytokine (interferon) secretion which aids in ROS generation, whereas the M2 phenotype is activated by interleukins possessing anti-inflammatory functions for repair processes (Huang et al. 2018; Oishi and Manabe 2018)

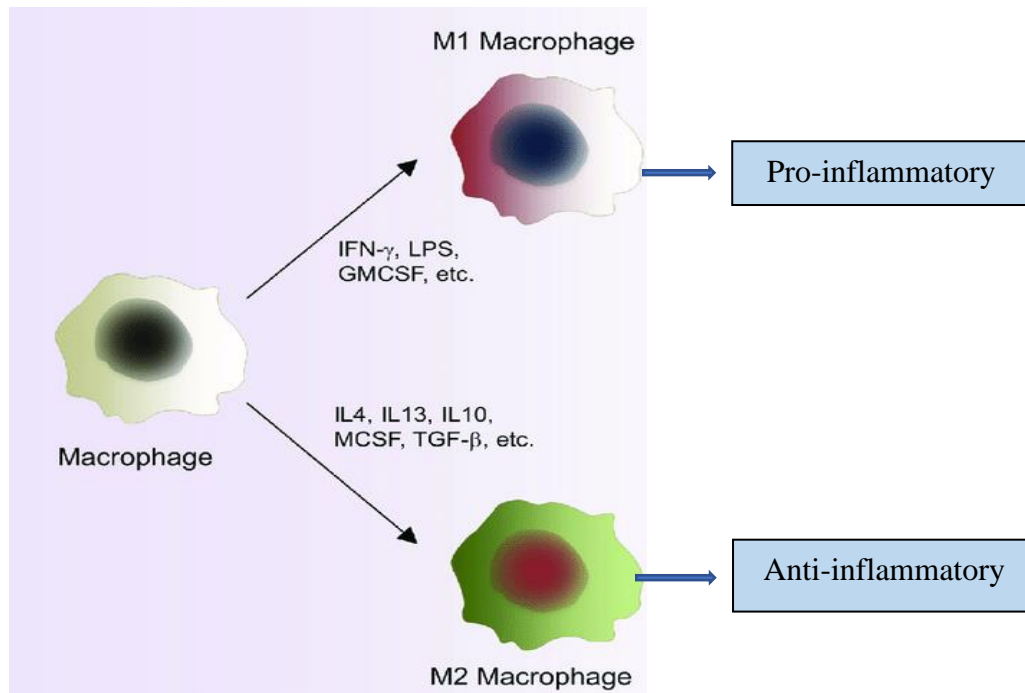


Figure 1. Macrophage polarization. M1 macrophages and M2 macrophages are pro-inflammatory and anti-inflammatory, respectively, each possessing the ability to secrete different cytokines (Saqib et al. 2018).

Macrophages polarize to these phenotypes by tightly regulated activation processes. M1 polarization is activated by the STAT1 pathway and M2 polarization is activated by the STAT3/STAT6 pathway. The balance between the two activation pathways is the key to the resulting inflammation state. Macrophages have the ability to transform to either phenotype depending on the environment (Parisi et al. 2018)



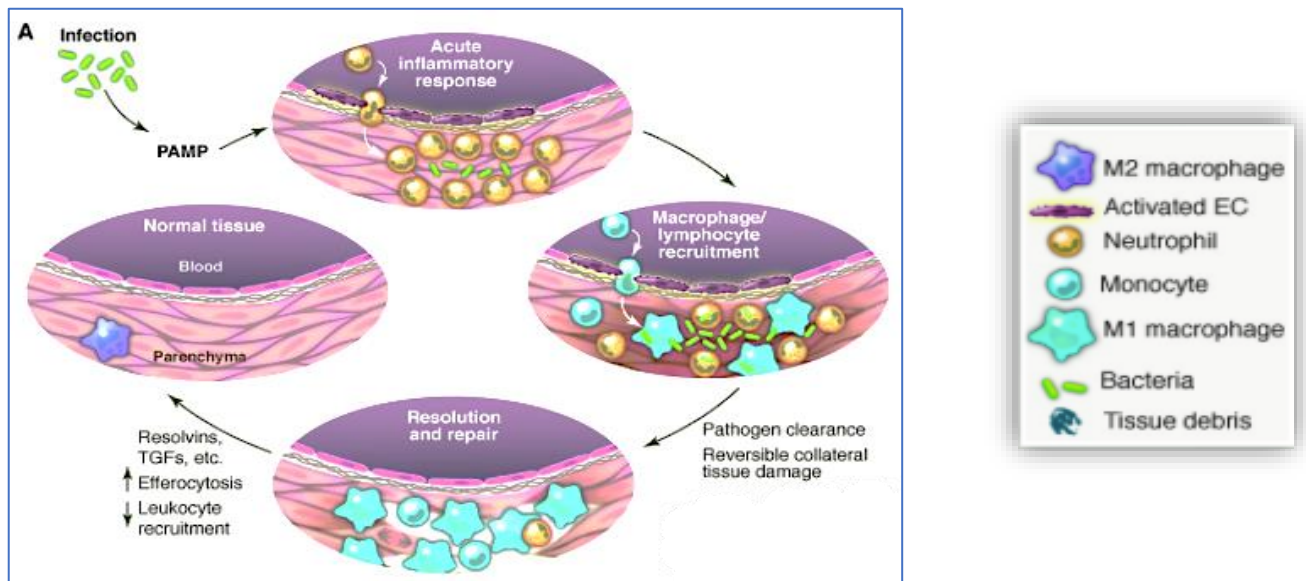


Figure 2. The acute inflammatory response to a bacterial infection. Reprinted with permission from the AAAS. Neutrophils infiltrate the infected tissue following the appearance of the inflammatory monocyte-derived macrophages. After the pathogen is cleared, the macrophage resolution and repair stage takes place until the parenchyma is restored (Odegaard and Chawla 2013).

### *Chronic Inflammation*

In response to trauma or a microbial invasion, short-term acute inflammation initially takes place to defend the host. However, the failure of acute inflammation to eradicate the pathogen results in inflammation for a longer period. Such persistent inflammation is called chronic inflammation, and this brings more serious pathological consequences. According to the World Health Organization (WHO), chronic diseases are the current greatest threat to human health. Three out of five people across the world die due to different chronic diseases such as cardiovascular disease, cancer, diabetes, obesity, etc. (Schett and Neurath 2018). Resolution of chronic inflammation can occur depending upon some important events, which mainly include the blockage of neutrophil recruitment, neutrophil apoptosis, and macrophage phenotype resolution (Schett and Neurath 2018). During chronic inflammation, anti-inflammatory and pro-inflammatory cytokines are both released for long period of time which leads to immunosuppression of the host (Rogovskii 2020). In the persistence of

inflammation, recruited macrophages accumulate in the tissue leading to the impairment of macrophage phenotypic switching, thereby disrupting the tissue microenvironment (Li et al. 2021).

*Correlation Between Chronic Inflammation and Macrophage Accumulation*

Unresolved acute inflammation and long-term leukocyte recruitment to the site of inflammation give rise to chronic inflammation. Specifically, inappropriate activation of macrophages leads to complex and abnormal outcomes such as rheumatoid arthritis, atherosclerosis, cancer, diabetes, etc. Macrophages have high plasticity allowing them to be diverse and multifunctional. Macrophages contribute to the initiation of chronic disease development (Liu et al. 2014). Macrophages act as a bridge between the innate and adaptive immune systems. Their involvement in chronic pathologies make them a therapeutic target (Song et al. 2022).

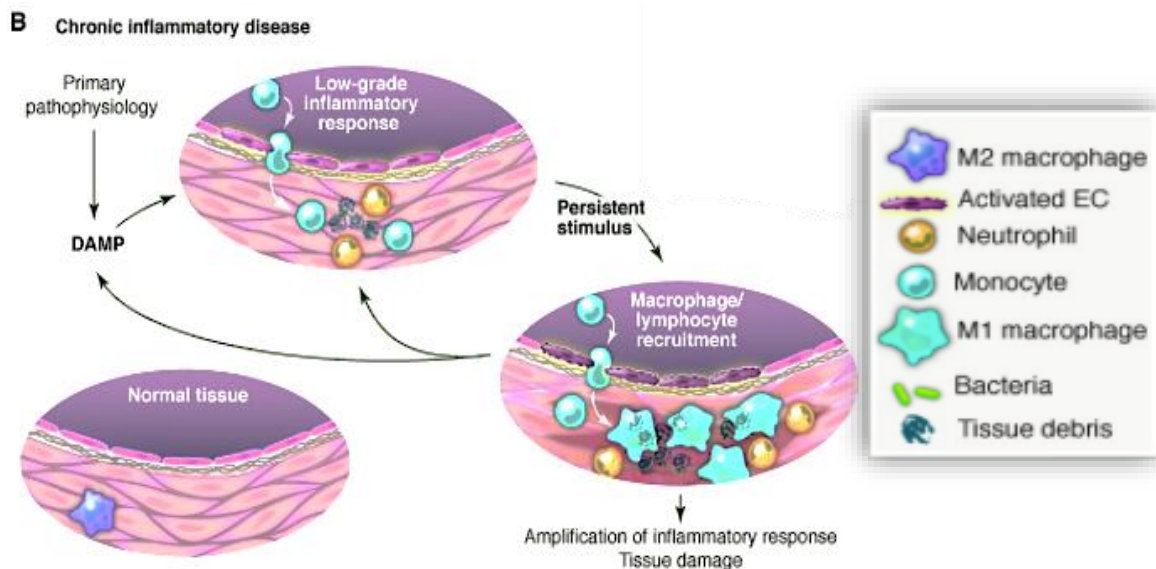


Figure 3. Chronic inflammation. Reprinted with permission from the AAAS. Chronic inflammations occur after acute inflammatory response is unable to clear pathogen. The persistent stimuli at the site of inflammation can lead to host tissue damage and different chronic diseases (Odegaard and Chawla 2013).

## *The Integrin Family*

Integrins are cell-adhesion receptors which play a vital role during developmental and in signalling different pathological pathways. The integrin family is composed of 24  $\alpha\beta$  heterodimeric members (Barczyk et al. 2010). Integrins are found in metazoans. Integrins have various functions in vertebrates ranging from cell-cell adhesion, regulating the cytoskeleton, cell migration, intracellular signalling, immune response, and tissue homeostasis (Hynes 1987).

### *Structure*

Integrins are cell adhesion heterodimeric receptors made of two subunits, an  $\alpha$ - and a  $\beta$ -subunits bound by non-covalent association. There are 18  $\alpha$ - and 8  $\beta$ -subunits comprising the 24 members of the human integrin superfamily (Berman et al. 2003). All integrins adopt a common shape consisting of a head, one upper leg, and one lower leg with one ligand-binding site. They have a larger extracellular portion, a small transmembrane domain, and a short cytoplasmic domain. Integrin  $\alpha$ - and  $\beta$ -subunits are very different with no obvious homology between them. Gene duplication events were responsible for the proliferation of the  $\alpha$ - and  $\beta$  gene families. Most of the chromosomes in humans contain at least one gene for an  $\alpha$ - or  $\beta$ -subunit. Each integrin member is dynamic in ligand binding and function. Their highly responsive receptor activation mechanism occurs due to changes in tertiary and quaternary structure following ligand binding (Takada et al. 2007).

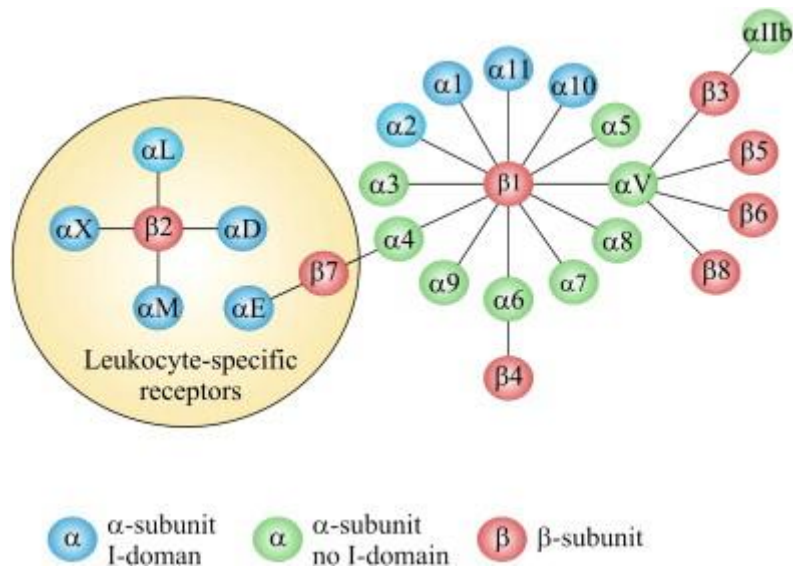


Figure 4. The integrin family consists of  $\alpha$  and  $\beta$ -subunits. Here leukocyte-specific receptors are shown (Gahmberg et al. 2009).

### *The Structure of Integrin Subunits*

The ligand specificity-determining  $\alpha$ -subunit of integrin is composed of a head, an upper leg, and a lower leg. The  $\alpha$ -subunit head contains a seven-bladed  $\beta$ -propeller connected to the thigh of the leg structure, which contains two more domains: calf-1 and calf-2. The leg structure supports the head structure. The EF-hand domain of the  $\beta$ -propeller facilitates  $Ca^{2+}$  binding. This binding has a regulatory effect on ligand binding. (Humphries 2003). There is one 180 amino acid-long inserted portion or I-domain between  $\beta$ -propeller blades 2 and 3. This inserted domain is present in nine of the total 18  $\alpha$ -subunits (Larson et al. 1989). Human  $\alpha_L$  ( $M_r$  177,000),  $\alpha_M$  ( $M_r$  165,000),  $\alpha_X$  ( $M_r$  150,000), and  $\alpha_D$  ( $M_r$  160,000) genes are in a cluster on chromosome 16. The sequences of these genes are 60-66% similar to  $\alpha_M$ ,  $\alpha_X$ , and  $\alpha_D$  and 35% similar to  $\alpha_L$  in terms of amino acid sequence. All of the above have a distal N-terminal extracellular 'I-domain' (inserted or interactive domain) (Harris et al. 2000).

Integrins containing  $\alpha$  I-domains show high homology in their I-domains. This characteristic makes the I-domain a very conserved region of integrins. In the I-domain, there is a Rossman fold surrounded by five  $\beta$ -sheets. There are seven  $\alpha$ -helices around these  $\beta$ -

sheets. The metal-ion-dependent adhesion site (MIDAS) motif of the I-domain contains a  $Mg^{2+}$  ion which facilitates ligand binding (Lee et al. 1995). The cytoplasmic domains of  $\alpha$ -subunits are quite diverse. It is assumed that the area connecting the  $\beta$  subunit and the  $\beta$ -propeller motif of the  $\alpha$  subunit is important for integrin heterodimerization. All  $\alpha$ -subunits and  $\beta$ -subunits are dimerized by the time they reach the plasma membrane (Humphries 2003).

The  $\beta$  subunit is quite different from the  $\alpha$  subunit containing a plexin-semaphoring-integrin (PSI) domain, a  $\beta$ I domain, a hybrid domain, and four cysteine-rich epidermal growth factor (EGF) repeats. Like in the  $\alpha$ I domain, the  $\beta$ I domain also contains a  $Mg^{2+}$  ion at MIDAS. Moreover, close to MIDAS, another site called ADMIDAS can bind a  $Ca^{2+}$  ion. This site is needed for conformational modification-mediated integrin activation. Integrins can transform to various conformations depending on how they are bend (Barczyk et al. 2010).

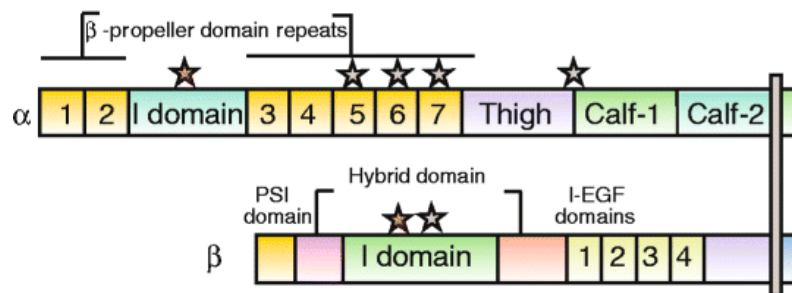


Figure 5. Representation of a prototypical  $\alpha$ I-domain-containing integrin heterodimer. Nine of the 18 integrin  $\alpha$ -chains contain an  $\alpha$ I-domain, as shown, but all integrins contain a  $\beta$ I domain in the  $\beta$  subunit. Representation of the domains in the  $\alpha$  I-domain-containing integrin (stars indicate divalent cation-binding sites) (Barczyk et al. 2010).

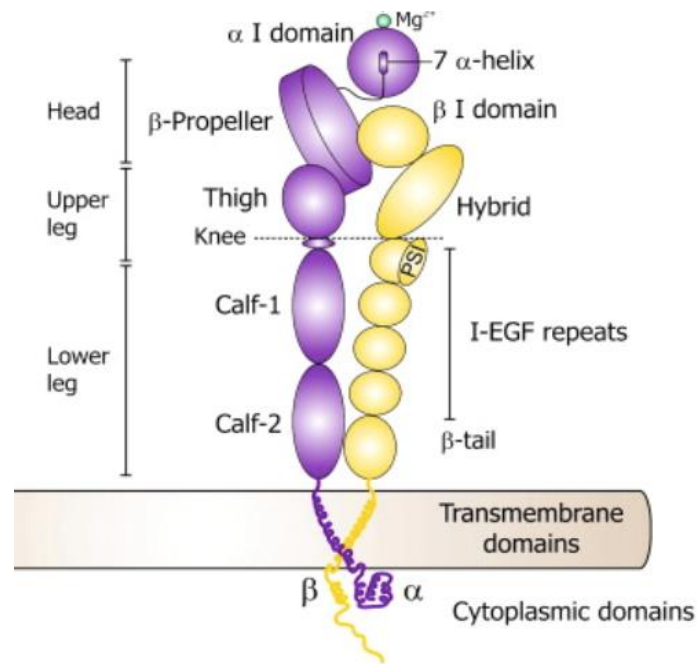


Figure 6. Structure of integrin. Integrins are heterodimers of an  $\alpha$ - subunit and a  $\beta$ -subunit bound together by non-covalent interactions. These heterodimers have a large extracellular portion (head and legs) and a small cytoplasmic domain (Gahmberg et al. 2009).

### *Integrin $\beta_2$*

The  $\beta_2$  integrins are one subfamily of the integrin family.  $\beta_2$  integrins are found only on leukocytes. Different leukocyte subpopulations express four types of  $\beta_2$  integrin dimers that play different immunological functions. Those four types of  $\beta_2$  integrin dimers are:  $\alpha_L\beta_2$  (CD11a/CD18; LFA-1),  $\alpha_M\beta_2$  (CD11b/CD18, MAC-1),  $\alpha_X\beta_2$  (CD11c/CD18), and  $\alpha_D\beta_2$  (CD11d/CD18).  $\alpha_L\beta_2$  is expressed on all leukocytes and can bind to ICAM ligands thereby facilitating cell-cell communication. This integrin has distinct structural properties compared with the others (Bouti et al. 2021).

Myeloid cells and neutrophils can express  $\alpha_M\beta_2$  (CD11b/CD18, MAC-1) and  $\alpha_X\beta_2$  (CD11c/CD18). On the other hand,  $\alpha_D\beta_2$  (CD11d/CD18) is expressed only on macrophages (Tan 2012). Integrins can be on a cell surface in three different conformations – bent-inactive, extended-inactive, or extended-active.  $\beta_2$  integrins expressed on leukocytes require kindlin-3 protein for ligand binding (Moser et al. 2009).  $\beta_2$  integrins are activated after recruitment of

additional proteins to the  $\beta_2$  integrin cytoplasmic tail.  $\beta_2$  integrins expressed on leukocytes play more downstream roles in signaling. These include chemokine-mediated signaling and selectin-mediated signaling, thereby facilitating inside-out signaling on the endothelium and conformational changes in  $\beta_2$  integrins. Inside-out signaling includes slow rolling, adhesion, and crawling. Later, the outside-in signaling starts with sensing of chemoattractant, polarization, and cell migration. These  $\beta_2$  integrin signal promotes leukocyte-mediated killing of pathogens, phagocytosis, as well as antibody-dependent cellular cytotoxicity. As  $\beta_2$  integrins expressed on leukocytes have various roles in the immune response and pathogenesis, focusing on  $\beta_2$  integrin functions could lead to the development of successful therapeutic approaches (Bouti et al. 2021). Figure 7 shows the bi-directional activation of integrins during leukocyte-endothelial cell interaction. Figure 8 shows the leukocyte adhesion cascade and its regulation by integrins (Ou et al. 2021).

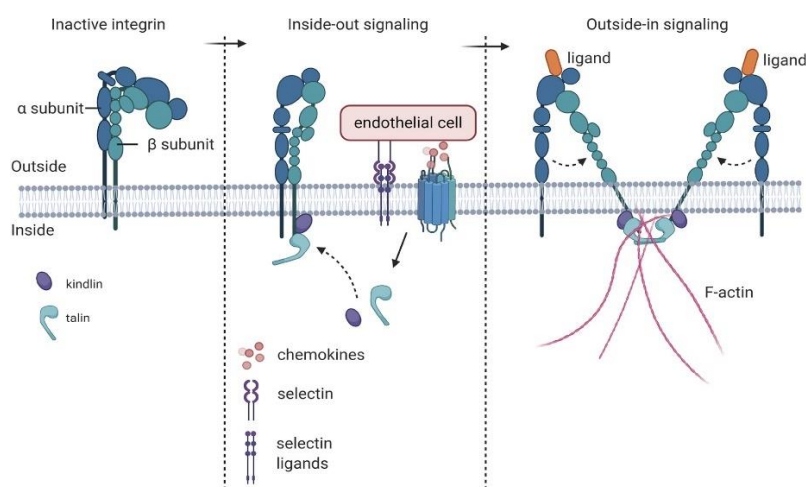


Figure 7. Bi-directional activation of integrins during leukocyte-endothelial cell interaction (Ou et al. 2021).

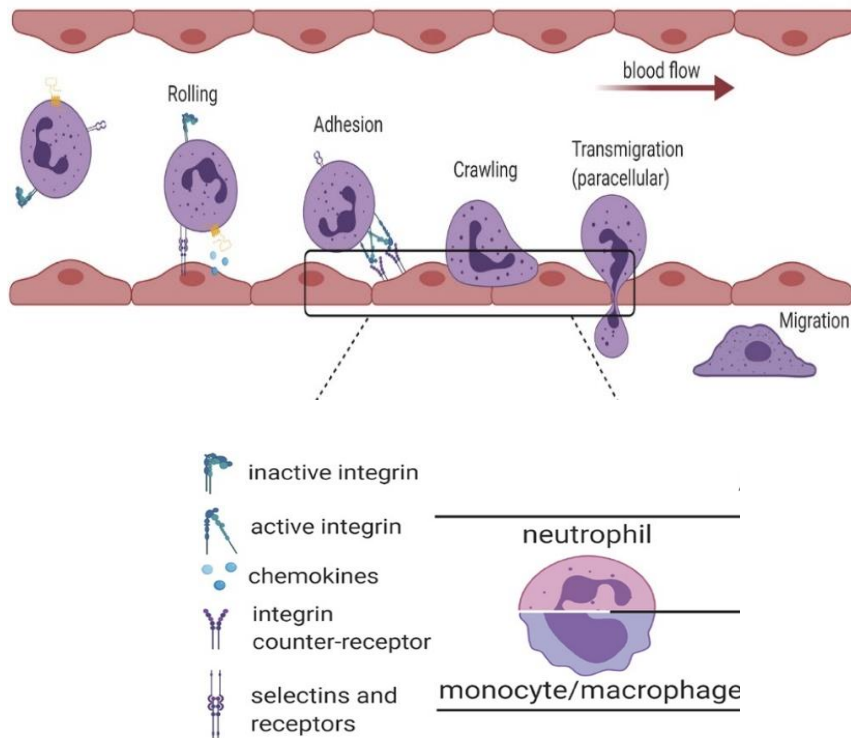


Figure 8. The leukocyte adhesion cascade and its regulation by integrins. This cascade is a multistep process consisting of rolling, adhesion, crawling, and migration of leukocytes through the endothelium to the site of inflammation mediated by different regulators (Ou et al. 2021).

### *Integrin $\alpha_D\beta_2$*

Integrin  $\alpha_D\beta_2$  is present on most leukocytes in the peripheral circulation. This integrin has been discovered relatively recently and its molecular characteristics indicate unique activation pathways and regulation. Integrin  $\alpha_D\beta_2$  is most highly expressed on macrophages. It is also expressed at lower levels on monocyte derived dendritic cells (DCs) and circulating monocytes. Its levels are increased during atherosclerosis, rheumatoid arthritis, acute lung inflammation, and other inflammatory injuries (Miyazaki et al. 2008). Integrin  $\alpha_D\beta_2$  has multi-ligand binding capacity. The ligands are mainly the ECM-associated proteins fibronectin, fibrinogen, vitronectin, Cyr61, plasminogen, ICAM-3, VCAM-1, etc. (Schittenhelm et al. 2017).

The most recently discovered ligand of integrin  $\alpha_D\beta_2$  is CEP (carboxyethyl pyrrole), which in turn can modify the ECM thereby generating CEP-modified proteins. It has been



shown that CEP-modified proteins trigger macrophage adhesion and migration to the site of inflammation (Yakubenko et al. 2018).

### *CEP- Integrin $\alpha_D\beta_2$ -Mediated Inflammation*

CEP is anticipated to be a useful marker of oxidative injuries in various tissue types. Understanding the pro-inflammatory mechanism of CEP is important because it is correlated with lipid-oxidation mediated human disease progression (Salomon et al. 2011). Macrophage migration to the site of inflammation is associated with oxidative modification of the ECM. It is assumed that polyunsaturated fatty acids (PUFAs) are oxidized by reactive oxygen species, which in turn produce different protein modifications such as CEP-modified proteins (Subbanagounder et al. 2000).

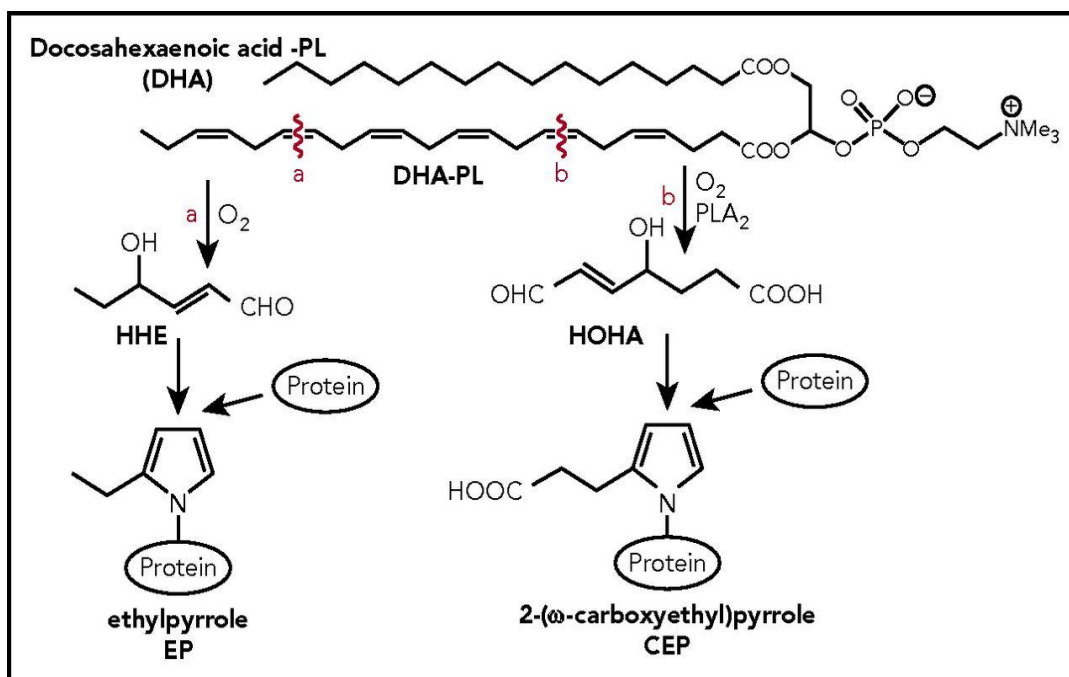


Figure 9. Generation of CEP and EP. DHA is a substrate of PLA<sub>2</sub>, thereby generating HOHA, which condenses with primary amino groups of protein lysyl residues and generates CEP–protein derivatives. Another structurally similar protein modification, ethylpyrrole (EP) is also generated. It is generated by alternative oxidative cleavage of DHA by producing 4-hydroxyhex-2-enal and condensing to 4-hydroxyhex-2-enal with the ε-amino group of lysyl residues. HHE, 4-hydroxyhexenal; HOHA, 4-hydroxy-7-oxo-hept-5-enoate (Yakubenko et al. 2018).

2-( $\omega$ -Carboxyethyl) pyrrole (CEP) is generated through adduction of the end products of docosahexaenoic acid (DHA) oxidation with the  $\epsilon$ -amino groups of protein lysyl residues. However, alternative oxidative cleavage of DHA produces another protein modification, ethyl pyrrole (EP) (Wang et al. 2015). It has been found that CEP plays a vital role in macrophage adhesion and migration to the site of inflammation (Yakubenko et al. 2018). Macrophages have unique receptors to bind to CEP-modified proteins.  $\alpha_D\beta_2$  and  $\alpha_M\beta_2$  integrins on macrophages are capable of binding to various ligands such as fibronectin, thrombospondin, vitronectin, etc. (Yakubenko et al. 2002). CEP adducts can bind to fibrinogen and CEP-modified fibrinogen has high affinity for  $\alpha_M\beta_2$  and  $\alpha_D\beta_2$  integrins, thereby making CEP-modified proteins a first priority ligand (Casteel et al. 2022). It was suggested that CEP can be involved in macrophage migration and macrophage retention. As the CEP-mediated macrophage accumulation is highly associated with various chronic inflammatory diseases, it is important to investigate how CEP-modified proteins interact with the I-domain of  $\alpha_D\beta_2$  integrins. The mapping of amino acids in the integrin  $\alpha_D$  I-domain might pave the way for a better understanding of inflammatory disease progression and severity. In fact, these ideas may help the development of new treatment approaches for inflammatory diseases in the future.

## CHAPTER 2. MATERIAL AND EXPERIMENTAL PROCEDURES

### *Materials*

All restriction enzymes, NEBuffer, Quick ligase, and Quick Ligase reaction buffer were purchased from New England BioLabs Inc. The QuickChange II site-directed mutagenesis kit was bought from Agilent Technologies. *PfuUltra* high fidelity DNA polymerase was included in the same mutagenesis kit. Competent cells were supplied by Thermo Fisher Scientific. For DNA isolation, QIAprep Spin miniprep kits were obtained from QIAGEN. All growth media were bought from MP Biomedicals, LLC. For protein purification, Thermo Scientific HisPur Ni-NTA Superflow Agarose was used. For protein analysis, a BCA Protein Assay Kit was purchased from Thermo Scientific and used. For biolayer interferometry, Amine Reactive (ARG2) ForteBio biosensor chips were used.

### *Experimental Procedure*

#### *Identification of Amino Acids for Mutation*

*Protein BLAST and 3D Protein Structure Prediction.* The  $\alpha_D$  I-domain amino acids were first analyzed before selecting a mutation site. For this purpose, NCBI protein BLAST was used and sequences of human  $\alpha_D$  I- domain and  $\alpha_M$  I-domain were compared. The gene IDs of human protein coding integrin subunit alpha D (ITGAD) and integrin subunit alpha M (ITGAM) are 3681 and 3684, respectively. Different bioinformatic software were used to predict the 3D- structure of  $\alpha_D$  I-domain before and after mutation. The FirstGlance program in Jmol software was used to locate selected amino acids of the  $\alpha_D$  I-domain and  $\alpha_M$  I-domain. Moreover, a 3D-structure of  $\alpha_D$  I-domain was created using SWISS model at those specific amino acid locations for both unmutated and mutated structures.

#### *Introduction of the Mutations*

*Recombinant Plasmid Generation.* Recombinant plasmid was generated using pET-28a as a vector and the human  $\alpha_D$  I-domain as the insert. For this purpose, the pET-28a

vector and the  $\alpha_D$  I-domain inserted in the pET-15b vector (preconstructed) were digested at restriction sites *NdeI* and *XhoI*, thereby creating sticky ends on both sequences. Moreover, the expression and cloning region in the maps for pET-28a vector also showed no additional sites for these restriction enzymes. Then the digestion reaction was performed by following the protocol recommended by the manufacturer (New England BioLabs Inc.). The components of the reaction were pipetted into two microcentrifuge tubes (one for vector and one for insert) as shown below in Table 1.

Table 1. Digestion reaction component with respective quantity

Components	Quantity/Volume
DNA	1 $\mu$ g
10X NEBuffer	5 $\mu$ l
Restriction enzyme ( <i>NdeI</i> and <i>XhoI</i> )	1 $\mu$ l each
Nuclease-free water	To 50 $\mu$ l

Then the solution was mixed gently by pipetting up and down. The reaction solution was incubated as well at 37°C for 5-15 minutes and heat inactivation was done at 65°C for exactly 20 minutes. Then the ligation was done using ligase in digestion reaction. For this purpose, the reaction was set up in a microcentrifuge tube on ice by following the protocol given by manufacturer (New England BioLabs Inc.). The components of the reaction were pipetted into a microcentrifuge tube as shown below in Table 2.

Table 2. Ligation reaction component with respective quantity

Components	20µl Reaction
Quick Ligase Reaction Buffer (2X)	10 µl
Vector DNA (4 kb)	50ng
Insert DNA (1 kb)	37.5ng
Nuclease-free water	Up to 20 µl
Quick Ligase	1 µl

Then the reaction was mixed gently by pipetting up and down and briefly spun down in a microfuge. The reaction was then incubated at room temperature for 5 minutes and stored at -20° C. In this way the  $\alpha_D$  I-domain was inserted into the vector for transcription by bacterial T7 polymerase. This polymerase is specific for the T7 promoter and the T7 terminator. The pET28a vector expression is under the control of the lac operon and the vector contains a kanamycin resistance gene.

*Generation of Mutagenic Primers.* Oligo software was used to generate mutagenic DNA primers. The upper and lower primer sequences used for generating each mutation are shown in the results section.

*PCR Site-Directed Mutagenesis.* QuikChange II Site-Directed Mutagenesis Kit was used to perform PCR site-directed mutagenesis (Agilent Technologies, Catalog # 200523). All components for the reaction were pipetted into a thin-walled PCR tube as shown below in Table 3.

Table 3. PCR sample reaction components for mutagenesis

Component	Quantity/Volume
10x Reaction Buffer	5 $\mu$ L
dsDNA Template	50 ng
Upper Mutagenic Oligonucleotide Primer	125 ng
Lower Mutagenic Oligonucleotide Primer	125 ng
dNTP Mix	1 $\mu$ L
ddH <sub>2</sub> O	To final volume of 50 $\mu$ L

After each of the sample reaction components were placed in the tube and gently mixed, 1 $\mu$ L of *PfuUltra* high fidelity DNA polymerase, provided in the QuickChange Kit, was added to the reaction. The sample reaction was then placed in a thermal cycler (BioRad T100) and cycled through the following conditions shown in Table 4 below as recommended by the Agilent Technologies, QuickChange II, site-directed mutagenesis kit.

Table 4. QuikChange II site-directed mutagenesis cycling conditions

Segment	Number of Cycles	Temperature	Time
1	1	95°C	30 seconds
2	18	95°C	30 seconds
		55°C	1 minute
		68°C	5 minutes 30 seconds
3	1	4°C	$\infty$

Each mutagenic construct created by PCR site-directed mutagenesis was cycled through the listed conditions. After the temperature cycling, the sample reaction was digested with 1 $\mu$ L of *DpnI* restriction enzyme by adding it directly. This digestion was done to remove

unmutated template from the PCR reaction. After mixing gently the reaction was incubated at 37°C for 1 hour.

*XL1-B Transformation.* For transformation, super-competent XL1-B cells were used following the manufacturer's protocol. For this purpose, the frozen XL1B cells were first thawed on ice for 30 minutes. Then 1uL of *DpnI*-treated DNA from the PCR sample reaction was added to the thawed cells. The transformation reaction mixture was gently flicked several times and placed on ice for 30 minutes. The transformation reaction was given heat-shock for exactly 20 seconds in a 42°C water bath and immediately placed on ice for a 2-minute incubation. Preheated 42°C SOC medium (Thermo Scientific, Catalog # 15544034) was added to the reaction. The mixture was then incubated at 37°C for 1 hour in an orbital shaker at 225 rpm. Petri dishes with LB-agar media were prepared by placing 32b LB-agar (Invitrogen by Life Technologies) in a liter of distilled water in a flask. Then the agar suspension was autoclaved for 15 minutes. After the autoclaving was done, the flask was cooled down below 50° C and then 100 ug/mL kanamycin was added, and the LB agar Petri dishes left to solidify. Once the incubation of the transformation reaction was completed, it was plated on the LB agar plates containing 100 ug/mL kanamycin and placed in a 37 °C incubator overnight. The next day, single colonies were observed and selected from the transformation plate. Then one colony was grown in 3 mL LB liquid medium containing 100 ug/mL kanamycin for 6 to 7 hours, diluted 1000 times and then cultured overnight. For the preparation of liquid LB media, 25g of LB-medium powder (MP Biomedicals, LLC) was added to 1L purified water. Then the medium was autoclaved for 15 minutes at 121°C.

*Recombinant Plasmid DNA Isolation.* From the grown culture, plasmid DNA was isolated by using the QIAprep Spin Miniprep Kit (Qiagen). According to instructions provided in the miniprep kit, 3 mL of bacterial cell culture was centrifuged in a table-top microcentrifuge by spinning at 8000 rpm for 3 minutes at room temperature. The supernatant

was discarded. The pelleted bacterial cells were resuspended in 250uL Buffer P1. After resuspension, buffer P2 was added and the sample was mixed by inverting the tube a few times. Then Buffer N3 was added and mixed immediately by inverting the tube for better mixing. Then the sample was placed in the microcentrifuge and spun for 10 minutes at 13,000 rpm. The supernatant was collected and transferred to a QIAprep 2.0 spin column 800uL at a time and centrifuged for 1 minute. Buffer PE was added to the spin column and then the spin column was centrifuged for 1 minute. The residual wash buffer was removed by centrifuging the column again for another minute. For DNA collection and elution, the spin column was transferred to a clean microcentrifuge tube and 30uL of preheated buffer EB was added to the center of the spin column. The column was then incubated at room temperature for 1 minute and then centrifuged for one minute at 13,000 rpm. The DNA concentration was determined using an absorbance reading on a microplate reader (Synergy H1 Hybrid Multi-Mode Microplate Reader, BioTek Instruments).

### *Protein Expression*

*BL21 Transformation.* Thermo scientific BL21(DE3) (catalog no. FEREC0114) competent cells were used for transforming the DNA following the manufacturer's instructions. At first the competent cells were thawed on ice for a few minutes. Then 50 ng of mutated plasmid DNA was added to the cells and mixed by flicking several times. The cells containing mutated DNA were then incubated on ice for 30 minutes. Once the incubation was done, the transformation reaction was heat-shocked for 45 seconds in a 42°C water bath. Then the reaction was immediately transferred on ice for exactly 2 minutes. Next, the preheated 37 °C sterile SOC medium was added to the cells. For growth, the cells were then incubated at 37°C for 1 hour in an orbital shaker at 225 rpm. After the incubation, the cells were plated on LB agar containing 100 ug/mL kanamycin and incubated at 37°C overnight.



*Cell Culture.* After growing overnight, the next morning the transformation plate was checked and from there a single colony was selected for growth. For the preparation of TB media, 50 g of Terrific Broth II powder (MP Biomedicals) was added to 1 L of purified water. Then the media was autoclaved at 121 °C for 15 minutes. Then the selected colony was transferred to a tube with 3 mL TB media containing 100 ug/mL kanamycin. The cells were cultured for 7-9 hours at 37 °C in a shaker rotating at 225 rpm. Then 100uL of the culture was transferred to 100 mL TB media and 100 ug/mL kanamycin and grown overnight. After growing overnight, the 100 mL of culture was brought up to 2 L by addition of 1.9 L of fresh TB media plus 100 ug/mL kanamycin. The 2 liters were split evenly between 4 flasks and cultured at 37°C with shaking for around 1.5 hours until the optical density reached around 0.9-1.

*Protein Expression with IPTG.* Recombinant protein expression was induced by addition of 1 mM isopropyl  $\beta$ -d-thiogalactopyranoside (IPTG) to the bacterial culture. Cells were incubated at 37 °C and 22 °C for mutant and wild type, respectively, in an orbital shaker rotating at 225 rpm for another 4 hours.

#### *Protein Isolation*

*Bacterial Cell Lysis.* After induction of protein expression, bacterial cell cultures were centrifuged at 6,000 rpm (3,951 RCF) and 4°C for 20 minutes. The supernatant was discarded and the bacterial cell pellet was lysed by resuspension in 1% Triton in PBS. The bacterial cell lysate was harvested and frozen overnight at -80°C. The next day, the bacterial lysate was thawed in a water bath for 20-30 minutes. The cells were then kept on ice and sonicated twice for two minutes intervals thereby destroying chromatin. After sonification, the suspension was spun down at 15,000 rpm for 30 minutes at 4°C to remove cellular debris. The supernatant containing the soluble protein was collected discarding the pellet. The supernatant was filtered using a 0.8 um syringe filter and stored in 50 ml tubes.

*Ni-NTA Column Chromatography.* Expressed proteins were isolated using Ni-NTA column chromatography. To stabilize the protein and block non-specific binding, imidazole and NaCl were added to the supernatant for a final concentration of 20 mM imidazole and 350 mM NaCl. Meanwhile, the Ni-NTA agarose was prepared by placing 1.5 ml agarose in a tube and adding 50ml of PBS. Then the Ni-NTA agarose was prepared by spinning at 1,000 rpm for 7 minutes. The supernatant containing the protein was then incubated with HisPur Ni-NTA Superflow Agarose (Thermo Scientific, Prod# 25214) at 4°C for 1 hour with gentle rocking. Once the incubation was done, the sample was spun 1,000 rpm at 4 °C for 10 minutes. The protein bound to Ni-NTA agarose was collected and transferred to a Poly-Prep chromatography column for isolation. After loading the Ni-NTA agarose bound to protein into the Poly-prep column, the column was washed. For washing different concentrations of imidazole (in 20 mM Tris pH 7.8) were prepared. The column was first washed with 20 ml 60 mM imidazole and then washed with 40 ml of 100 mM imidazole. While washing the OD of the eluent was measured to check if it reached less than 0.1. Washing continued until the OD was less than 0.1. Then, the elution steps started. For elution 250 mM imidazole was used. The concentration of eluted protein was measured using a spectrophotometer. The samples with the highest protein concentrations were collected for dialysis.

*Protein Dialysis.* The selected pre-dialysis protein samples were placed in dialysis tubing (Fisherbrand # 21-152-10). There are two dialysis steps. At first the dialysis tubing was kept in 1X PBS and 500 mM NaCl and dialyzed for 30 minutes at 4°C with gentle stirring. Then the dialysis buffer was renewed and dialyzed overnight. The next day the protein-containing tubing was placed into 500 mL of 150 mM NaCl plus 20mMHepes with two changes every 5 hours at 4°C with gentle stirring. Then the post-dialyzed protein samples were collected from the tubing and concentrations were measured using a spectrophotometer. Protein aliquots were prepared in smaller tubes for freezing and later use.

### *Protein Analysis*

*SDS-PAGE.* Protein was analyzed by performing SDS-PAGE. SDS-PAGE is a good way for protein visualization and purification. For each sample, 10uL of 5x SDS loading buffer was added to a 40uL protein sample. The protein samples were denatured for 5 minutes at 100 °C. For SDS-PAGE, a 15% polyacrylamide gel was prepared. The protein molecular weight markers (Precision Plus Protein™ Dual Color Standards, 500 µl #1610374, BioRad) were loaded in the first well of the gel. Blank samples were added to the next two wells. Then all prepared samples were sequentially loaded into the rest of the wells. After performing gel electrophoresis, the gel was washed with a fixing solution (10% acetic acid, 50% methanol, and 40% water). Then the staining solution containing Coomassie blue R250, Coomassie blue G250, amido black, 90% water, and 10% acetic acid was used to stain the gel. After staining, the de-staining solution was used for proper band visualization.

*BCA Assay.* A way to measure protein concentration is a BCA assay for which the BCA Protein Assay Kit (Thermo Scientific) was used. Standards from 0 ug/mL to 2,000 ug/mL of bovine serum albumin (BSA) were provided with the kit and diluted with buffer containing 150mM NaCl and 20mMHepes. Then, 25uL of each standard or protein sample were added to individual wells of a 96 well plate (Immulon, 2HB). After adding standards and samples into the wells of the plate, 200 uL of working reagent provided by the kit was added to each well containing a standard or sample. The working reagent was prepared using solutions A and B in a 4:1 proportion. The plate was incubated at 37°C for 30 minutes after shaking for exactly 30 seconds. Following incubation, the plate was allowed to cool and the absorbance at 562 nm was measured by using the Synergy H1 Hybrid Multi-Mode Microplate Reader from BioTek Instruments. A standard curve was generated by evaluating the absorbance and known concentrations of each standard. Microsoft Excel was used for

data analysis. The concentration of protein in each sample was calculated using the generated standard curve from the linear regression.

### *Biolayer Interferometry*

By using biolayer interferometry, the binding affinities of wild type  $\alpha_D$  I-domain protein and mutant  $\alpha_D$  I-domain protein to CEP were assessed with the ForteBio K2 Octet system.

*Amine Reactive (ARG2) Biosensor Assays.* For assessment, Amine Reactive (ARG2) ForteBio biosensor chips were used to test protein interaction with CEP. At first, CEP-BSA was immobilized on the Amine Reactive Second-generation (AR2G) biosensor using the amine coupler kit. The protective surface of the ARG2 biosensor was removed by soaking in buffer containing 150 mM NaCl and 20mMHepes. ARG2 biosensor activation was performed with N-hydroxysulfosuccinimide (s-NHS) and 1-ethyl-3-(3-(dimethylamino) propyl) carbodiimide (EDC). The ligands were then placed in sodium acetate solution adjusted to pH 6 and immobilized onto the activated biosensor surface. Quenching of unreacted sites on the biosensor surface was performed with 1 M ethanolamine. Proteins were assayed in buffer containing 150mM NaCl, 20mMHepes, 1 mM CaCl<sub>2</sub>, 1mM MgCl<sub>2</sub>, and 0.05% Tween-20. The value of the equilibrium dissociation constant ( $K_D$ ) was obtained by fitting a plot of response at equilibrium ( $R_{eq}$ ) against the concentrations.

### *Experimental Design Flow Through*

Analyze amino acids of  $\alpha_D$  I-domain involved in binding to CEP-modified proteins and 3D structure prediction of  $\alpha_D$  I-domain using NCBI BLAST and SWISS model



Generate recombinant plasmid for the expression of mutated I-domain in *E. Coli* and verify the  $\alpha_D$  I-domain presence in it



Design the mutagenic primer using Oligo software and generate the mutant construct by a 3-step PCR-site directed mutagenesis



Express the mutated proteins through molecular cloning and test their binding to CEP-modified protein through ForteBio



Analyze the protein-protein binding affinity of CEP-modified protein to WT  $\alpha_D$  I-domain and mutant  $\alpha_D$  I-domain

## CHAPTER 3. RESULTS

### *Selection of $\alpha_D$ I-Domain Amino Acids Important for Binding to CEP*

This research of thesis aimed to identify the amino acids of integrin  $\alpha_D\beta_2$  which facilitated binding to CEP-modified proteins. The I-domain of the  $\alpha_D$  subunit is the major site for ligand binding. It is important to analyze the amino acids of this domain which might be required for chronic inflammatory pathway activation to develop specific inhibitors as anti-inflammatory drugs, thereby obstructing macrophage accumulation at the site of inflammation. A comparative BLAST analysis was done which compared the amino acid sequences of the  $\alpha_D$  and  $\alpha_M$  subunits. The results showed that these two subunits have 60% homology. Some positively charged amino acids at the I-domain of the  $\alpha_D$  subunit were chosen having a high probability of binding the negatively charged P5 peptide, which does not bind to the  $\alpha_M$  subunit. This concept provided the rationale for selecting seven amino acids for primary analysis (Figure 10).

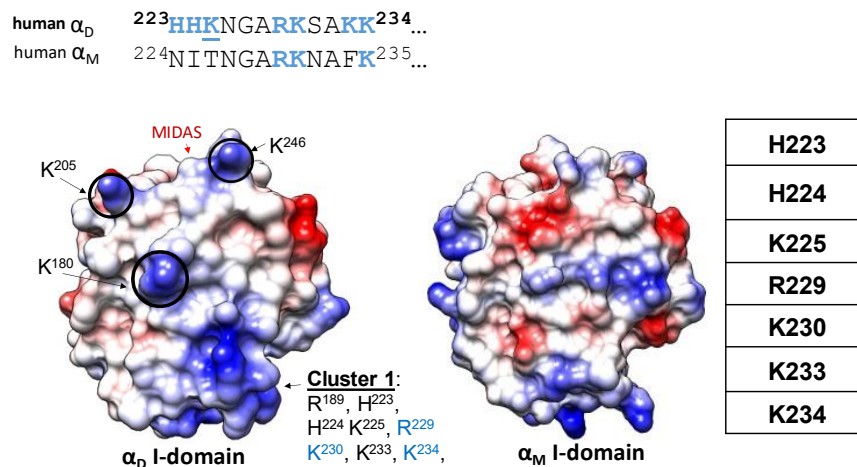


Figure 10. NCBI BLAST analysis and structure prediction of the integrin  $\alpha_D$  I-domain.

Figure 10 also depicts the structure of the  $\alpha_M$  I-domain and the  $\alpha_D$  I-domain. The structure of the  $\alpha_M$  I-domain was already solved. I used this generated structure to predict the location of selected amino acids in the I-domain of the  $\alpha_D$  subunit. For this process, the FirstGlance program

in Jmol software was used. The  $\alpha_M$  structural model was downloaded using PDB identification code 1IDO. Then each selected amino acid location was investigated to determine the respective amino acid location in the  $\alpha_D$  subunit. For further experiments such as site directed mutagenesis, seven positively charged amino acids were chosen. Those were H223, H224, K225, R229, K230, K233, K234. Table 5 below shows the process that was used for selecting the  $\alpha_D$  I-domain amino acids intended for mutagenesis.

Table 5. Selection process of  $\alpha_D$  I-domain amino acids for mutagenesis

$\alpha_D$ I-domain amino acids selected for potential analysis	Identification Method		Corresponding amino acid in $\alpha_M$	Selected for Analysis
	$\alpha_M$ BLAST	Predicted $\alpha_D$ Structure		
<b>H223</b>	✓	✓	N223	✓
<b>H224</b>	✓	✓	I224	✓
<b>K225</b>	✓	✓	T225	✓
<b>R229</b>	✓	✓	R229	✓
<b>K230</b>	✓	✓	K230	✓
<b>K233</b>	✓	✓	F233	✓
<b>K234</b>	✓	✓	K234	✓

Along with the FirstGlance program in the Jmol software, another software SWISS-MODEL was used to create an automated comparative model of 3D protein structure. But this was applied only for specific areas of the  $\alpha_D$  I-domain where mutagenesis was to occur. From this bioinformatics analysis it was clear that the ligand binding area was predicted to maintain a

similar structure before and after mutagenesis. It is important to have similar structural characteristics to facilitate the binding of inflammatory ligands. Figure 11 shows the predicted structures before mutation, where the mutagenic area starts from His240 and ends at Lys251 and after mutation, where the mutagenic area starts at Asn240 and ends at Ala251.

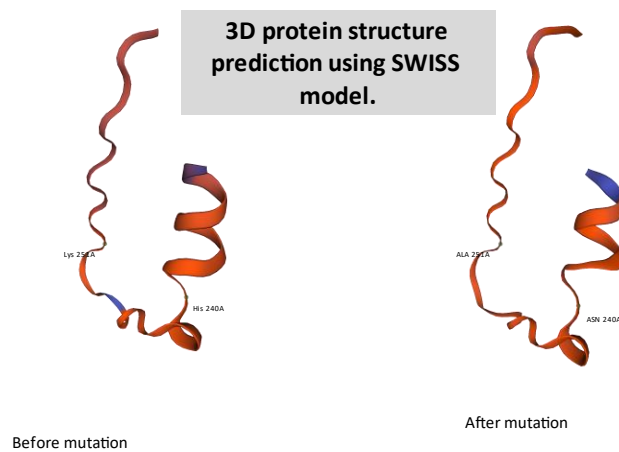


Figure 11. Prediction using SWISS model of the  $\alpha_D$  I-domain structure before and after mutation. The structure shows no significant changes in 3D structure of the  $\alpha_D$  I-domain fragment when the mutations are introduced.



## Recombinant Plasmid Generation

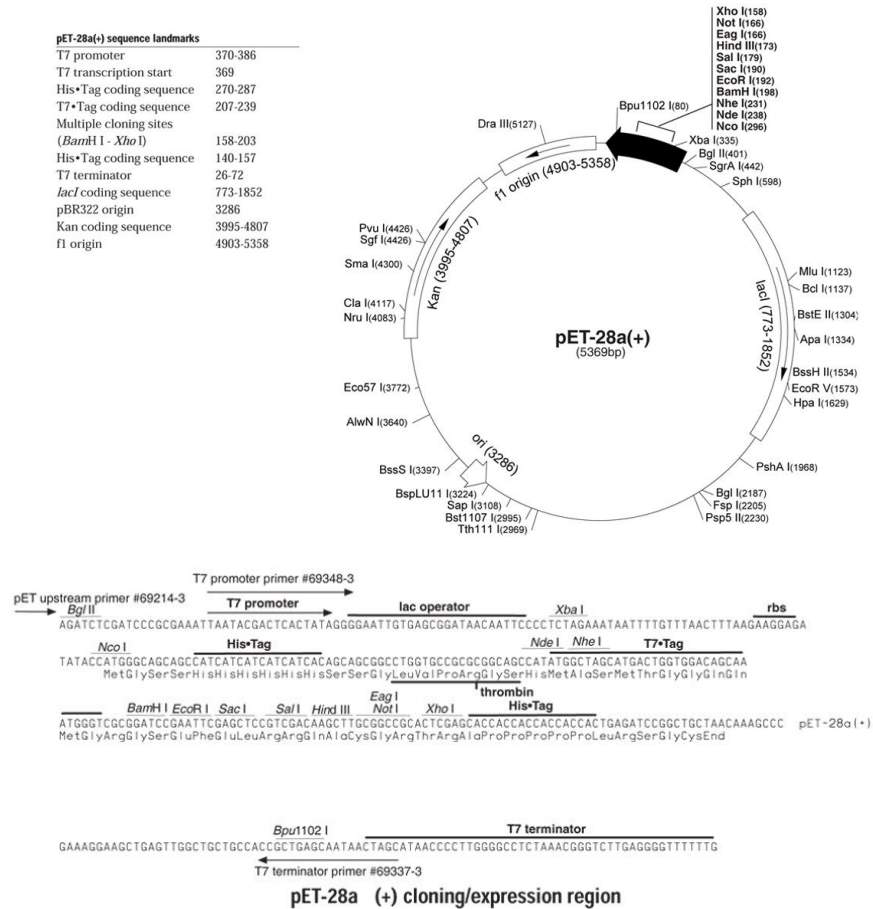


Figure 12. The pET-28a(+) vector. It carries an N-terminal His•Tag/thrombin/T7•Tag configuration in addition to an optional C-terminal His•Tag sequence.

To create recombinant plasmid, the 5369 bp pET-28a vector carries an N-terminal His.Tag/Thrombin/T7 sequence as well as a C-terminal His tag was used. The multiple cloning site spans bps 158 to 203. The cloning region is transcribed by T7 RNA polymerase. Sequencing can be performed using a T7 terminator primer. So, this vector seemed quite compatible for molecular cloning. It is commonly used to express His-tagged protein with high efficiency (Figure12).

### Verification of the Presence of the $\alpha_D$ I-Domain in the pET28a Vector

pET28a and the  $\alpha_D$  I-domain both were digested at two common sites, *NdeI* and *XhoI*, which later were ligated and transformed into DH5 $\alpha$  competent cells. Following DNA isolation, the recombinant  $\alpha_D$  I-domain was sequenced facilitated by the presence of the presence of the T7 DNA polymerase promoter. The sequencing results showed that the recombinant plasmid contained both cloning sites. However, to further verify the presence of the  $\alpha_D$  I-domain in pET28a, a digestion with only *XhoI* was performed to linearize the plasmid. After electrophoresis, the digestion reaction showed an approximately 6,000bp long band on the DNA gel, the correct length for the plasmid with the inserted  $\alpha_D$  I-domain.

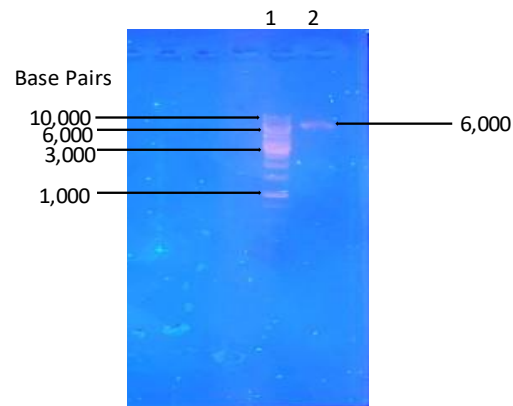


Figure 13. Verification of the presence of the  $\alpha_D$  I-domain in pET28a using a single restriction enzyme. The digestion reaction showed a band on the DNA agarose gel, which was around 6,000bp. The image was taken using a UV transilluminator. Lane 1: the DNA ladder, Lane 2: the restriction reaction.

Moreover, to confirm the presence of the  $\alpha_D$  I-domain in pET28a, a PCR reaction was performed. The figure below shows the result of the DNA agarose gel electrophoresis after the PCR reaction on the recombinant plasmid  $\alpha_D$ -pET28a. This PCR used  $\alpha_D$ -upper and  $\alpha_D$ -lower

primers. The resulting fragment length was around the expected 600 bp. It is known that the  $\alpha_D$  fragment is about 600 bp. So, the band on the gel depicts the expected result.

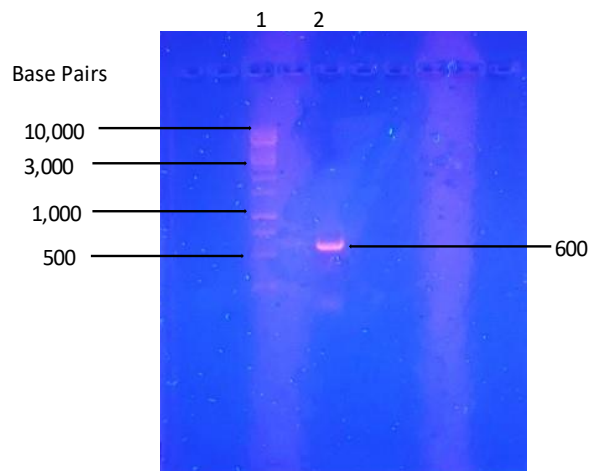


Figure 14. Verification of the presence of the  $\alpha_D$  I-domain in pET28a using PCR of the insert. The digestion reaction shows a band on the DNA agarose gel which is around 600 bp compared to the 10,000 bp DNA ladder. The image was taken using a UV transilluminator. Lane 1: DNA ladder, Lane 2: PCR product.

#### *Primer Design and Mutant Construct Generation*

In total 7 amino acids were chosen for PCR site-directed mutagenesis. This mutagenesis was performed sequentially resulting in one final mutant of human  $\alpha_D$  I-domain protein. At first K233 and K234 (located in tandem) were chosen and changed to A233 and G234 amino acids. The next mutagenesis was done on another group of sequential amino acids. This substitution was from H223, H224, and K225 to N223, I224, and T225. The third mutagenesis was performed changing R229 and K230 to G229 and A230. In all, seven positively charged amino acids of the human  $\alpha_D$  I-domain were changed. To create these mutations to the expected DNA substitutions, mutagenic DNA primers were first generated with the help of Oligo software. This software was very helpful for making mutagenic DNA primers by calculating the GC content, the melting temperature, the molecular weight etc. It also assesses potential primer dimerization

and identifies potential secondary structures. In the following table, mutant position, amino acid substitution, DNA base substitution, upper mutagenic primer sequence and lower mutagenic primer sequences are shown.

Table 6. Mutagenic construct generation using the newly designed primers

Mutant	Amino Acid Substitution	DNA Base Substitution	Upper Primer Sequence	Lower Primer Sequence
KK233-234	KK233-234 → AG233-234	CAAGAAG →AGCAGGA	5'- GGGGCCCCGA AAAAGTGCAGC AGGAATCCTCA TTGTCATC-3'	5'- GATGAC AAT GAGGATTCCTGCT GCACT TTT TCG GGC CCC 3'
HHK223-225	HHK 223-225 → NIT 223-225	CATCATAAG → AATATTACG	5'- GGTGACACAGC TATTTAATATTA CGAATGGGGCC CGAAAAAG-3'	5'- CTTTTTCGGGCCCC ATTCGTAATATTA AATAGCTGTGTCA CC-3'
RK229-230	RK229-230 → GA229-230	AGGAAG → GGCGCT	5'- ATTACGAATGG GGCCGGCGCTA GTGCAGCAGGG ATC-3'	5'- GATCCCTGCTGCA CTAGCGCCGGCCC CATTCGTAAT-3'

#### *First Mutation Generation*

To perform the first PCR site-directed mutagenesis from KK233-234 to AG233-234, the  $\alpha_D$ -PET28a recombinant plasmid was used. In the figure, the agarose gel was supposed to show a band at approximately 6000 bp containing the mutant plasmid. But it didn't show up as expected, although Figure 16 from Oligo Software analysis showed the presence of mutated

amino acids with no additional alterations in the isolated DNA sequence. The DNA may have been degraded.

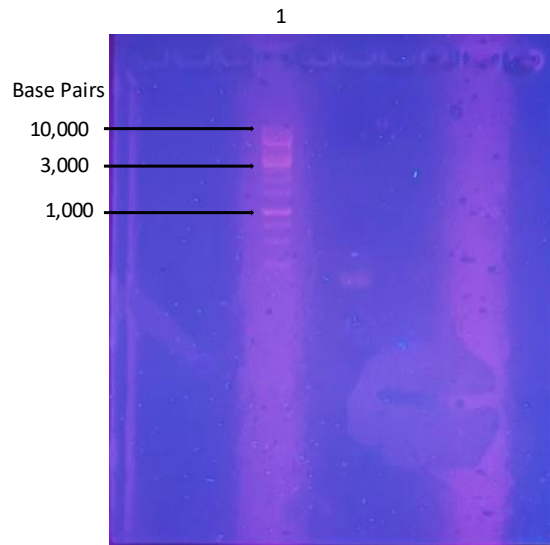


Figure 15. DNA gel electrophoresis of isolated mutant DNA after the first PCR site-directed mutagenesis. This gel didn't show the expected band at around the 6,000 bp position. Lane 1: DNA ladder. Lane 2: plasmid DNA

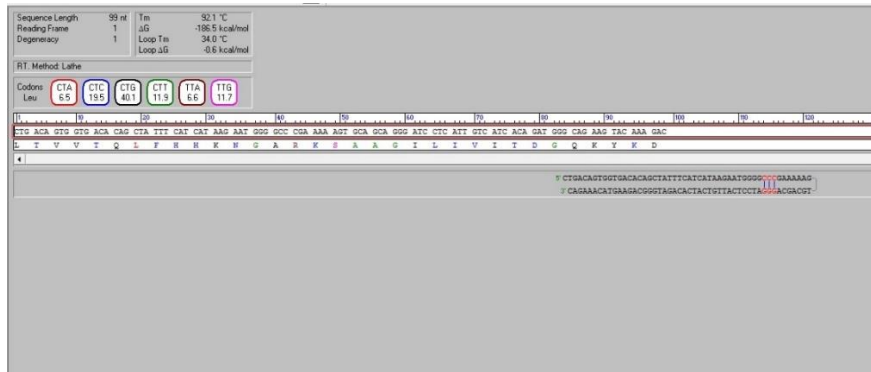


Figure 16. The first DNA mutation was confirmed using Oligo Software. This software showed the presence of the A233 and G234 mutations in the isolated DNA sequence.

### *Second Mutation Generation*

Then second PCR site-directed mutagenesis was performed to change amino acids HHK 223-225 to NIT 223-225, where the plasmid created in the first mutagenesis experiment was used as the template instead of the  $\alpha_D$ -PET28a recombinant plasmid. In Figure 17, the agarose gel shows the expected band size at approximately 6,000 bp as expected for the mutant. Moreover, this result was confirmed when Oligo Software analysis directly showed the presence of the expected mutated amino acids with no additional alterations in the DNA sequence (Figure 18).

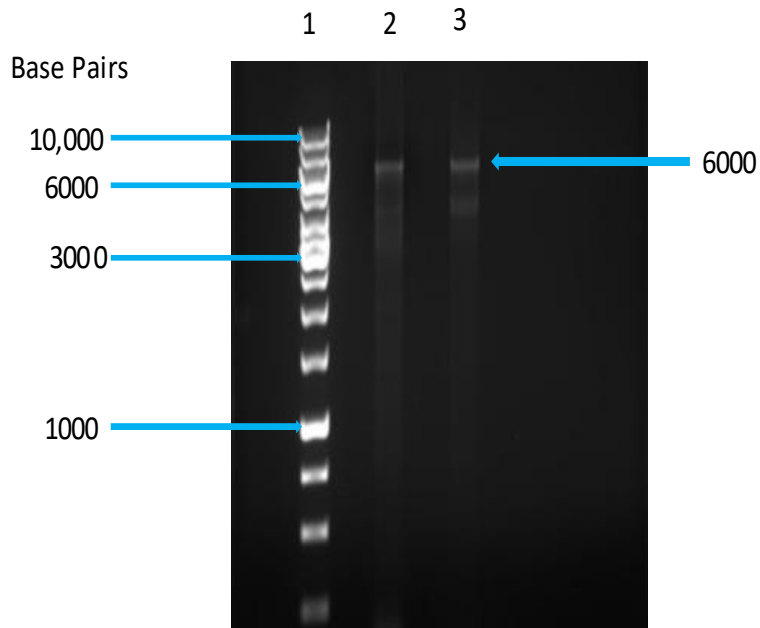


Figure 17. DNA gel electrophoresis of isolated mutant DNA after the second PCR site-directed mutagenesis. Here the first mutant was used as the template. This gel electrophoresis showed the expected band at around the 6,000 bp position compared to the DNA ladder. This suggests that the mutations were introduced at the correct sites. Lane 1: DNA ladder, Lane 2 and Lane 3:  $\alpha_D$  I-domain mutant.

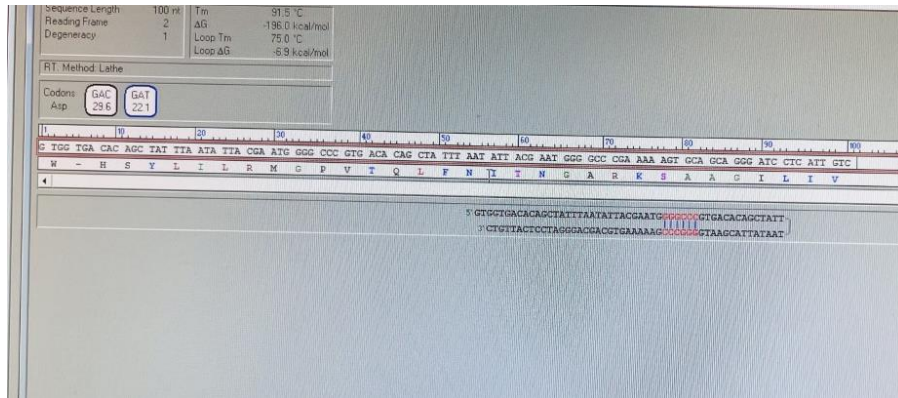


Figure 18. Confirmation of the success of the second DNA mutagenesis experiment. Oligo Software was used to confirm the introduction of the N223, I224 and T225 mutations in the isolated DNA sequence.

### *Third Mutation Generation (RK to GA)*

In the same way the third mutagenesis experiment was performed with PCR site-directed mutagenesis changing RK229-230 to GA229-230, where the resultant plasmid from the second mutagenesis experiment was used as the template. As shown in Figure 19, the agarose gel shows the expected band size at approximately 6,000 bp containing all DNA mutations to cause the seven amino acid substitutions. Likewise, this result was verified using Oligo Software sequence analysis, which showed the presence of the expected mutated bases with no additional alterations in the DNA sequence (Figure 20).

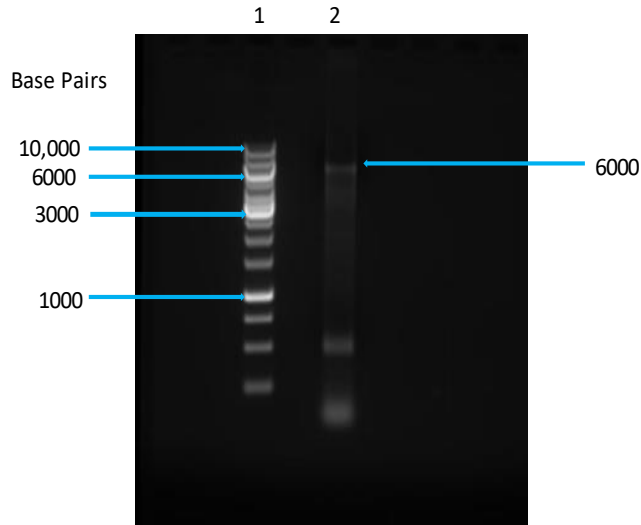


Figure 19. DNA gel electrophoresis of isolated mutant DNA after the third PCR site-directed mutagenesis experiment. Here, the second mutant was used as the template. This gel electrophoresis showed the expected band at around the 6000 bp position compared to the DNA ladder showing that the mutation did not alter the length of the DNA. Lane 1: DNA ladder, Lane 2:  $\alpha_D$  I-domain mutant.

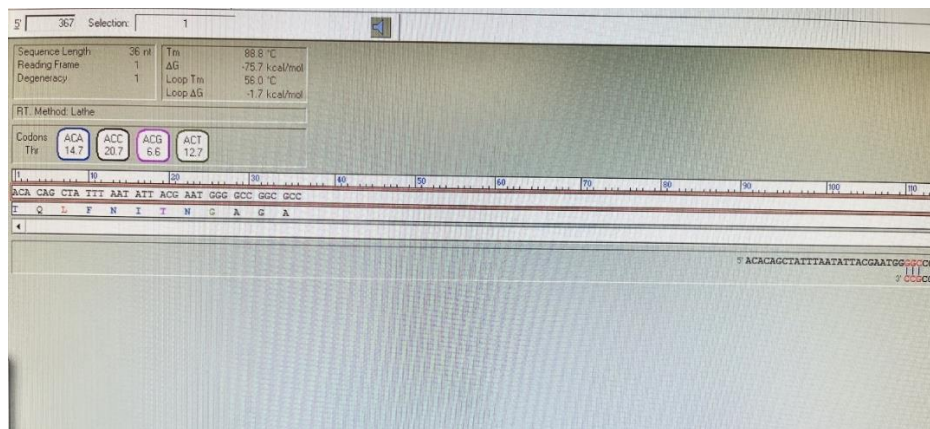


Figure 20. The third and final DNA mutagenesis step was confirmed. Oligo Software sequence analyzer was used to show the presence of the introduced mutations in the isolated DNA sequence.



### *The Final Sequence of the Mutated $\alpha_D$ I-Domain*

After completing the three steps of PCR-site directed mutagenesis, the final mutant  $\alpha_D$  I-domain with seven amino acid mutations was generated. The fragment of interest of the mutant  $\alpha_D$  I-domain was altered from <sup>223</sup>HHKNGARKSAKK<sup>234</sup> to <sup>223</sup>NITNGAGASAAG<sup>234</sup>.

### *Protein Purification and Analysis*

With the substitution of seven amino acids in the  $\alpha_D$ -I domain, the mutant  $\alpha_D$  I-domain construct was finally finished. So, both wild-type (control) and mutant (test sample)  $\alpha_D$  I-domain were transformed into *E. coli* BL21 cells. After culturing the cells in TB media, protein expression was induced by the addition of IPTG. For  $\alpha_D$  I-domain protein isolation, Ni-NTA affinity chromatography was used. After isolation, the collected protein sample underwent a 2-step dialysis with changes in buffer concentrations.

The concentration of the isolated wild-type and mutant  $\alpha_D$  I-domain protein was determined by performing a BCA protein assay and found to be 72 ug/mL and 68 ug/mL, respectively. Protein was analyzed by running wild-type and mutant  $\alpha_D$  I-domain protein samples using sodium dodecyl-sulfate polyacrylamide electrophoresis (SDS-PAGE) with a 12% agarose gel. The image of the stained gel after running the SDS-PAGE is shown below in Figure 21.

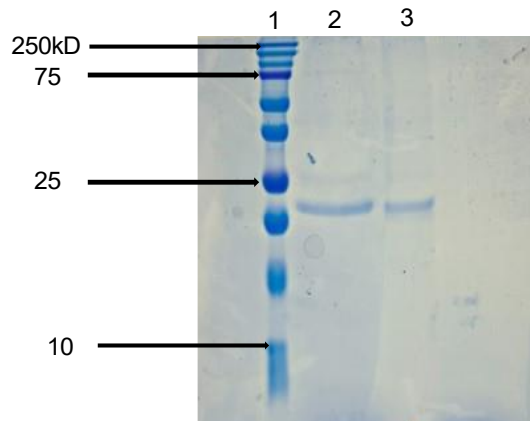


Figure 21. SDS-polyacrylamide gel electrophoresis (12%) for isolated WT and mutant  $\alpha_D$  I-domain proteins. Lane 1: Protein standards. Lane 2: Post-dialysis WT I-domain. Lane 3: Post-dialysis  $\alpha_D$  I-domain mutant.

*The  $\alpha_D$  I-domain Mutant Demonstrated a Reduction in Binding to CEP Compared to the Wild-Type  $\alpha_D$  I-Domain*

After confirming the concentration of WT and mutant  $\alpha_D$  I-domain protein by the BCA protein determination assay, a protein-protein binding assay was performed. For this experiment, different concentrations of WT and mutant  $\alpha_D$  I-domain protein were used to test their ability to bind to CEP by a ForteBio Octet Protein-Protein binding assay. CEP was first immobilized onto an Amine Reactive ARG2 biosensor and the I-domain binding to CEP was measured in real time. Figure 22 shows that the level of WT I-domain binding markedly exceeds the binding of mutant  $\alpha_D$  I-domain to CEP. Therefore,  $\alpha_D$  region H<sup>223</sup>-K<sup>234</sup> contains amino acids which are likely involved in the binding to CEP.

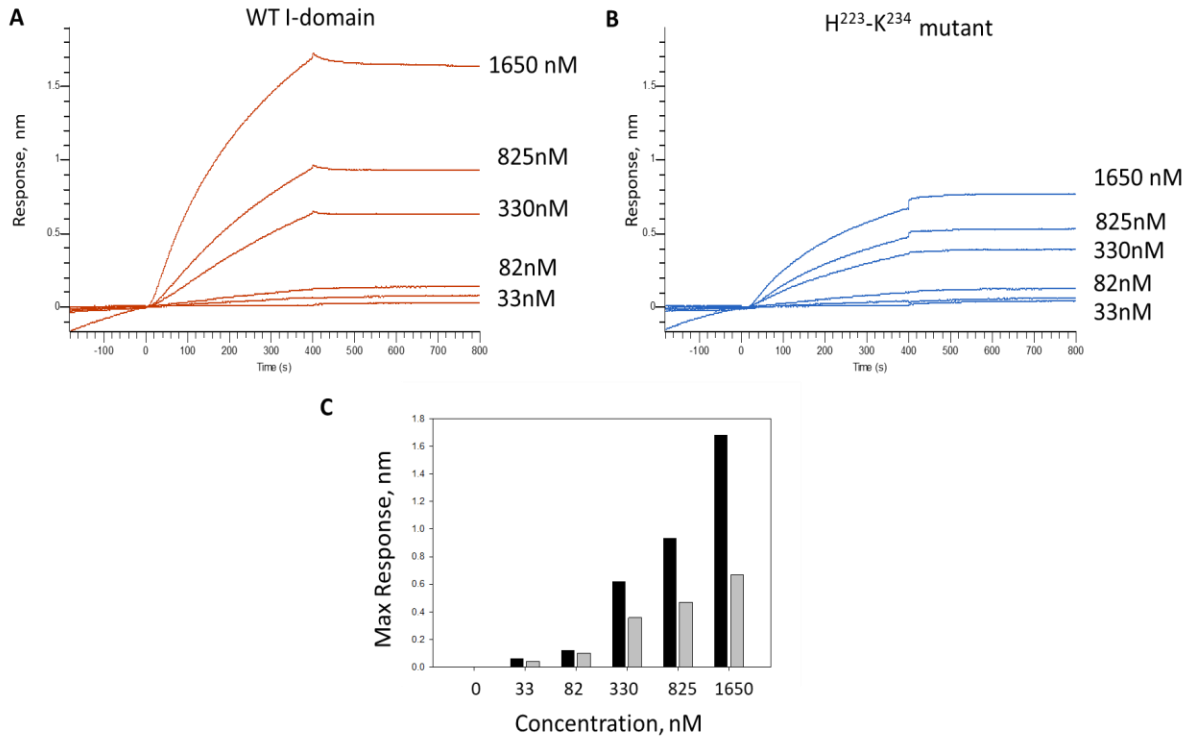


Figure 22. WT and mutant  $\alpha_D$  I-domain binding to CEP. Representative ForteBio Octet Protein-Protein assay sensorgram of WT  $\alpha_D$  I-domain (A) and H<sup>223</sup>-K<sup>234</sup> mutant  $\alpha_D$  I-domain (B) binding to immobilized CEP on an Amine-Reactive Arginine biosensor. The association between the I-domain and CEP takes place from time 0 to 400 seconds followed by dissociation until 800 seconds. (C) The bar chart displays the comparison of the maximum response of WT  $\alpha_D$  I-domain and the H<sup>223</sup>-K<sup>234</sup> mutant  $\alpha_D$  I-domain to CEP at different concentrations. At every concentration, WT  $\alpha_D$  I-domain had a greater maximum response than the mutant  $\alpha_D$  I-domain. (Grey bar: mutant  $\alpha_D$  I-domain and black bar: WT  $\alpha_D$  I-domain).

## CHAPTER 4. DISCUSSION

In response to various pathogens, the immune system recruits different types of leukocytes to the site of inflammation. But the persistent recruitment of leukocytes, specifically macrophages, to the site of inflammation leads to many chronic diseases such as diabetes, obesity, atherosclerosis, cancer, arthritis, etc. It has been found that macrophage-specific receptor, integrin  $\alpha_D\beta_2$ , plays an important role in such accumulation and recruitment to the site of inflammation. During the early stages of inflammation, recruited neutrophils cause oxidation by secreting peroxidases. These peroxidases oxidize the polyunsaturated fatty acids (PUFAs) of the ECM thereby producing 2-( $\omega$ -carboxyethyl) pyrrole (CEP)-modified proteins, which have an increased negative charge due to the carboxyl group in CEP. Moreover, at the site of inflammation, macrophages co-localize with CEP. So, it is very important to investigate how integrin  $\alpha_D\beta_2$  of macrophages binds to CEP-modified proteins. Therefore, basic amino acid residues in the  $\alpha_D$  I-domain, which are not shared with other related integrin family members, were chosen and mutated to better understand the binding characteristics of the  $\alpha_D$  I-domain to CEP. So, the main purpose of this thesis was to identify a role for positively charged amino acids in integrin  $\alpha_D\beta_2$  in the binding to CEP-modified proteins. By performing comparative analysis with NCBI BLAST, I found that the amino acid sequences of  $\alpha_D$  and  $\alpha_M$  subunits had 60% homology. This information was important for predicting the 3D- structure of the  $\alpha_D$  I-domain and selecting the amino acids to mutate. After the selection process, the  $\alpha_D$  I-domain structures before and after mutation were predicted using SWISS model software. The results predicted that the intended mutation in the  $\alpha_D$  I-domain did not result in significant changes in the loop structure. Such integrity in loop structure is necessary for active binding of ligands or inhibitors.

Another challenge of the experimental plan was the generation of the recombinant plasmid by inserting the DNA sequence of the  $\alpha_D$  I-domain into the 5369 bp pET-28a vector between the two restriction sites, *NdeI* and *XhoI*. Before starting restriction digestion, all sequence landmarks of this vector were intensively analyzed to understand its compatibility to express the fusion protein. A PCR reaction and a restriction digestion were both conducted to verify the presence of the  $\alpha_D$  I-domain in the pET28a vector. In both cases following DNA agarose gel electrophoresis, the expected band results were visualized.

Mutagenic primer design was another critical step in the PCR site-directed mutagenesis protocol. Three mutagenic primers were designed considering optimum loop temperature, length, mutation, and location. After the three-step mutagenesis, one  $\alpha_D$  I-domain mutant containing the seven amino acid alteration was finally obtained. Every step of the mutagenesis process was analyzed and confirmed in two ways. First, confirmation was performed by DNA gel electrophoresis, which showed the expected approximate size of mutant vector on the gel. Second, confirmation was performed by sequencing the DNA, which showed the correct mutation was present in the correct location in the sequence with minimal contamination and impurity. These procedures led to the precise mutant generation for further analysis.

Both wild type and mutant  $\alpha_D$  I-domain proteins with poly-histidine tags were expressed in the BL21 *E. coli* strain and isolated using Ni-agarose chromatography. Upon analyzing protein purification by SDS-PAGE, the concentration was evaluated using BCA assay and spectrophotometry. The SDS-PAGE results showed that both proteins ran on the gel as bands at the expected position with a similar molecular weight (~21,000 Da). The good purity of the isolated proteins and the sufficient concentration allowed us to use these proteins for binding assays to CEP.

Then, ForteBio Octet protein-protein binding assays were performed to analyse the importance of the positively-charged cluster H<sup>223</sup>-K<sup>234</sup> within the integrin  $\alpha_D$  structure for the binding to CEP. Therefore, the binding properties of WT  $\alpha_D$  and the H<sup>223</sup>-K<sup>234</sup> mutant were compared. In this project, the positively charged His-tagged sequence was not removed from the proteins, which could possibly enhance the binding to the negatively charged carboxyl group of CEPs. Previously in my lab  $\alpha_D\beta_2$ -transfected HEK293 cells were generated which showed enhanced cell adhesion. Moreover, the protein-protein binding interaction between  $\alpha_D$  I-domain and CEP was also measured. These experiments already demonstrated that  $\alpha_D\beta_2$  had a strong binding affinity toward CEP-modified proteins and the negative charge of carboxyl group present in CEP was required for this strong interaction. The initial results and analysis and from this project showed that WT  $\alpha_D$  I-domain protein had a considerably higher binding affinity for CEP than the mutant  $\alpha_D$  I-domain protein. The result of this experiment supports my hypothesis. Such differences highlight the role of these selected positively charged amino acids (<sup>223</sup>HHKNGARKSAKK<sup>234</sup>) in binding to negatively charged CEP. The CEP binding site within the  $\alpha_D$  I-domain may therefore be a good target for developing blocking antibodies to prevent adhesion of macrophages to CEP-modified proteins and to alleviate the macrophage retention at the site of chronic inflammation. Thus, the information about this site generated by my research may one day help prevent or delay chronic inflammatory diseases like diabetes, obesity, or cardiovascular diseases. Therefore, the findings from this thesis are of great importance for the development of treatments against chronic diseases. However, more experiments are needed to fully understand integrin  $\alpha_D\beta_2$ -CEP interactions before clinical therapies can be developed.

## REFERENCES

- Ai Z, Udalova IA. 2020. Transcriptional regulation of neutrophil differentiation and function during inflammation. *J Leukoc Biol.* 107(3):419–430. doi:10.1002/JLB.1RU1219-504RR.
- Barczyk M, Carracedo S, Gullberg D. 2010. Integrins. *Cell Tissue Res.* 339(1):269–280. doi:10.1007/s00441-009-0834-6.
- Bashir S, Sharma Y, Elahi A, Khan F. 2016. Macrophage polarization: the link between inflammation and related diseases. *Inflamm Res.* 65(1):1–11. doi:10.1007/s00011-015-0874-1.
- Berman AE, Kozlova NI, Morozevich GE. 2003. Integrins: Structure and Signaling. *Biochem Mosc.* 68(12):1284–1299. doi:10.1023/B:BIRY.0000011649.03634.74.
- Bouti P, Webbers SDS, Fagerholm SC, Alon R, Moser M, Matlung HL, Kuijpers TW. 2021.  $\beta$ 2 Integrin Signaling Cascade in Neutrophils: More Than a Single Function. *Front Immunol.* 11. <https://www.frontiersin.org/articles/10.3389/fimmu.2020.619925>.
- Brostjan C, Oehler R. 2020. The role of neutrophil death in chronic inflammation and cancer. *Cell Death Discov.* 6(1):1–8. doi:10.1038/s41420-020-0255-6.
- Casteel JL, Keever KR, Ardell CL, Williams DL, Gao D, Podrez EA, Byzova TV, Yakubenko VP. 2022. Modification of Extracellular Matrix by the Product of DHA Oxidation Switches Macrophage Adhesion Patterns and Promotes Retention of Macrophages During Chronic Inflammation. *Front Immunol.* 13:867082. doi:10.3389/fimmu.2022.867082.
- Chen L, Deng H, Cui H, Fang J, Zuo Z, Deng J, Li Y, Wang X, Zhao L. 2017. Inflammatory responses and inflammation-associated diseases in organs. *Oncotarget.* 9(6):7204–7218. doi:10.18632/oncotarget.23208.
- Chow CC, Clermont G, Kumar R, Lagoa C, Tawadrous Z, Gallo D, Betten B, Bartels J, Constantine G, Fink MP, et al. 2005. THE ACUTE INFLAMMATORY RESPONSE IN DIVERSE SHOCK STATES. *Shock.* 24(1):74. doi:10.1097/01.shk.0000168526.97716.f3.
- Davignon J-L, Hayder M, Baron M, Boyer J-F, Constantin A, Apparailly F, Poupot R, Cantagrel A. 2013. Targeting monocytes/macrophages in the treatment of rheumatoid arthritis. *Rheumatology.* 52(4):590–598. doi:10.1093/rheumatology/kes304.

- Freire MO, Van Dyke TE. 2013. Natural resolution of inflammation. *Periodontol* 2000. 63(1):149–164. doi:10.1111/prd.12034.
- Gahmberg CG, Fagerholm SC, Nurmi SM, Chavakis T, Marchesan S, Grönholm M. 2009. Regulation of integrin activity and signalling. *Biochim Biophys Acta BBA - Gen Subj*. 1790(6):431–444. doi:10.1016/j.bbagen.2009.03.007.
- Harris ES, McIntyre TM, Prescott SM, Zimmerman GA. 2000. The Leukocyte Integrins\*. *J Biol Chem*. 275(31):23409–23412. doi:10.1074/jbc.R000004200.
- Huang X, Li Y, Fu M, Xin H-B. 2018. Polarizing Macrophages In Vitro. In: Rousselet G, editor. *Macrophages: Methods and Protocols*. New York, NY: Springer New York. p. 119–126. [https://doi.org/10.1007/978-1-4939-7837-3\\_12](https://doi.org/10.1007/978-1-4939-7837-3_12).
- Humphries M. 2003. Mapping functional residues onto integrin crystal structures. *Curr Opin Struct Biol*. 13(2):236–243. doi:10.1016/S0959-440X(03)00035-6.
- Hynes R. 1987. Integrins: A family of cell surface receptors. *Cell*. 48(4):549–554. doi:10.1016/0092-8674(87)90233-9.
- Kaplanski G. 2003. IL-6: a regulator of the transition from neutrophil to monocyte recruitment during inflammation. *Trends Immunol*. 24(1):25–29. doi:10.1016/S1471-4906(02)00013-3.
- Kumar R, Clermont G, Vodovotz Y, Chow CC. 2004. The dynamics of acute inflammation. *J Theor Biol*. 230(2):145–155. doi:10.1016/j.jtbi.2004.04.044.
- Larson RS, Corbi AL, Berman L, Springer T. 1989. Primary structure of the leukocyte function-associated molecule-1 alpha subunit: an integrin with an embedded domain defining a protein superfamily. *J Cell Biol*. 108(2):703–712. doi:10.1083/jcb.108.2.703.
- Lee J-O, Bankston LA, Robert C Liddington MAA and. 1995. Two conformations of the integrin A-domain (I-domain): a pathway for activation? *Structure*. 3(12):1333–1340. doi:10.1016/S0969-2126(01)00271-4.
- Li M, Hou Q, Zhong L, Zhao Y, Fu X. 2021. Macrophage Related Chronic Inflammation in Non-Healing Wounds. *Front Immunol*. 12. <https://www.frontiersin.org/articles/10.3389/fimmu.2021.681710>.
- Liu Y-C, Zou X-B, Chai Y-F, Yao Y-M. 2014. Macrophage Polarization in Inflammatory Diseases. *Int J Biol Sci*. 10(5):520–529. doi:10.7150/ijbs.8879.



- McLoughlin RM, Hurst SM, Nowell MA, Harris DA, Horiuchi S, Morgan LW, Wilkinson TS, Yamamoto N, Topley N, Jones SA. 2004. Differential Regulation of Neutrophil-Activating Chemokines by IL-6 and Its Soluble Receptor Isoforms<sup>1</sup>. *J Immunol.* 172(9):5676–5683. doi:10.4049/jimmunol.172.9.5676.
- Meizlish ML, Franklin RA, Zhou X, Medzhitov R. 2021. Tissue Homeostasis and Inflammation. *Annu Rev Immunol.* 39(1):557–581. doi:10.1146/annurev-immunol-061020-053734.
- Miyazaki Y, Bunting M, Stafforini DM, Harris ES, McIntyre TM, Prescott SM, Frutuoso VS, Amendoeira FC, de Oliveira Nascimento D, Vieira-de-Abreu A, et al. 2008. Integrin  $\alpha$ D $\beta$ 2 Is Dynamically Expressed by Inflamed Macrophages and Alters the Natural History of Lethal Systemic Infections<sup>1</sup>. *J Immunol.* 180(1):590–600. doi:10.4049/jimmunol.180.1.590.
- Moser M, Bauer M, Schmid S, Ruppert R, Schmidt S, Sixt M, Wang H-V, Sperandio M, Fässler R. 2009. Kindlin-3 is required for  $\beta$ 2 integrin–mediated leukocyte adhesion to endothelial cells. *Nat Med.* 15(3):300–305. doi:10.1038/nm.1921.
- Odegaard JI, Chawla A. 2013. Pleiotropic Actions of Insulin Resistance and Inflammation in Metabolic Homeostasis. *Science.* 339(6116):172–177. doi:10.1126/science.1230721.
- Oishi Y, Manabe I. 2018. Macrophages in inflammation, repair and regeneration. *Int Immunol.* 30(11):511–528. doi:10.1093/intimm/dxy054.
- Ou Z, Dolmatova E, Lassègue B, Griendling KK. 2021.  $\beta$ 1- and  $\beta$ 2-integrins: central players in regulating vascular permeability and leukocyte recruitment during acute inflammation. *Am J Physiol-Heart Circ Physiol.* 320(2):H734–H739. doi:10.1152/ajpheart.00518.2020.
- Parisi L, Gini E, Baci D, Tremolati M, Fanuli M, Bassani B, Farronato G, Bruno A, Mortara L. 2018. Macrophage Polarization in Chronic Inflammatory Diseases: Killers or Builders? *J Immunol Res.* 2018:1–25. doi:10.1155/2018/8917804.
- Ponzoni M, Pastorino F, Di Paolo D, Perri P, Brignole C. 2018. Targeting Macrophages as a Potential Therapeutic Intervention: Impact on Inflammatory Diseases and Cancer. *Int J Mol Sci.* 19(7):1953. doi:10.3390/ijms19071953.

- Prame Kumar K, Nicholls AJ, Wong CHY. 2018. Partners in crime: neutrophils and monocytes/macrophages in inflammation and disease. *Cell Tissue Res.* 371(3):551–565. doi:10.1007/s00441-017-2753-2.
- Rankin JA. 2004. Biological Mediators of Acute Inflammation. *AACN Adv Crit Care.* 15(1):3–17.
- Rogovskii V. 2020. Immune Tolerance as the Physiologic Counterpart of Chronic Inflammation. *Front Immunol.* 11. <https://www.frontiersin.org/articles/10.3389/fimmu.2020.02061>.
- Salomon RG, Hong L, Hollyfield JG. 2011. Discovery of Carboxyethylpyrroles (CEPs): Critical Insights into AMD, Autism, Cancer, and Wound Healing from Basic Research on the Chemistry of Oxidized Phospholipids. *Chem Res Toxicol.* 24(11):1803–1816. doi:10.1021/tx200206v.
- Saqib U, Sarkar S, Suk K, Owais M, Baig M, Savai R. 2018. Phytochemicals as modulators of M1-M2 macrophages in inflammation. *Oncotarget.* 9. doi:10.18632/oncotarget.24788.
- Schett G, Neurath MF. 2018. Resolution of chronic inflammatory disease: universal and tissue-specific concepts. *Nat Commun.* 9(1):3261. doi:10.1038/s41467-018-05800-6.
- Schittenhelm L, Hilkens CM, Morrison VL. 2017.  $\beta$ 2 Integrins As Regulators of Dendritic Cell, Monocyte, and Macrophage Function. *Front Immunol.* 8. <https://www.frontiersin.org/articles/10.3389/fimmu.2017.01866>.
- Schmid-Schönbein GW. 2006. Analysis of Inflammation. *Annu Rev Biomed Eng.* 8(1):93–151. doi:10.1146/annurev.bioeng.8.061505.095708.
- Song Y, Huang Y, Zhou F, Ding J, Zhou W. 2022. Macrophage-targeted nanomedicine for chronic diseases immunotherapy. *Chin Chem Lett.* 33(2):597–612. doi:10.1016/j.ccllet.2021.08.090.
- Subbanagounder G, Leitinger N, Schwenke DC, Wong JW, Lee H, Rizza C, Watson AD, Faull KF, Fogelman AM, Berliner JA. 2000. Determinants of Bioactivity of Oxidized Phospholipids. *Arterioscler Thromb Vasc Biol.* 20(10):2248–2254. doi:10.1161/01.ATV.20.10.2248.
- Sugimoto MA, Vago JP, Perretti M, Teixeira MM. 2019. Mediators of the Resolution of the Inflammatory Response. *Trends Immunol.* 40(3):212–227. doi:10.1016/j.it.2019.01.007.

- Takada Y, Ye X, Simon S. 2007. The integrins. *Genome Biol.* 8(5):215. doi:10.1186/gb-2007-8-5-215.
- Takeuchi O, Akira S. 2010. Pattern Recognition Receptors and Inflammation. *Cell.* 140(6):805–820. doi:10.1016/j.cell.2010.01.022.
- Tan S-M. 2012. The leucocyte  $\beta 2$  (CD18) integrins: the structure, functional regulation and signalling properties. *Biosci Rep.* 32(3):241–269. doi:10.1042/BSR20110101.
- Voisin M-B, Nourshargh S. 2013. Neutrophil Transmigration: Emergence of an Adhesive Cascade within Venular Walls. *J Innate Immun.* 5(4):336–347. doi:10.1159/000346659.
- Wang H, Linetsky M, Guo J, Choi J, Hong L, Chamberlain AS, Howell SJ, Howes AM, Salomon RG. 2015. 4-Hydroxy-7-oxo-5-heptenoic Acid (HOHA) Lactone is a Biologically Active Precursor for the Generation of 2-( $\omega$ -Carboxyethyl)pyrrole (CEP) Derivatives of Proteins and Ethanolamine Phospholipids. *Chem Res Toxicol.* 28(5):967–977. doi:10.1021/acs.chemrestox.5b00001.
- Williams MR, Azcutia V, Newton G, Alcaide P, Luscinskas FW. 2011. Emerging mechanisms of neutrophil recruitment across endothelium. *Spec Issue Innate Immune Cell Traffick.* 32(10):461–469. doi:10.1016/j.it.2011.06.009.
- Yakubenko VP, Cui K, Ardell CL, Brown KE, West XZ, Gao D, Stefl S, Salomon RG, Podrez EA, Byzova TV. 2018. Oxidative modifications of extracellular matrix promote the second wave of inflammation via  $\beta 2$  integrins. *Blood.* 132(1):78–88. doi:10.1182/blood-2017-10-810176.
- Yakubenko VP, Lishko VK, Lam SC-T, Ugarova TP. 2002. A Molecular Basis for Integrin  $\alpha M\beta 2$  Ligand Binding Promiscuity \*. *J Biol Chem.* 277(50):48635–48642. doi:10.1074/jbc.M208877200.

VITA

AFIA MAHEDA PREMA

- Education: M.S. Biology, East Tennessee State University, Johnson  
City, Tennessee, 2023
- B.Sc. Biochemistry and Molecular Biology, Shahjalal University of  
Science and Technology, Sylhet, Bangladesh, 2019
- Professional Experience: Graduate Teaching Assistant, East Tennessee State  
University, Department of Biological Sciences, 2021-2023
- Honors and awards: Certificate of Achievement in 8<sup>th</sup> and 7<sup>th</sup> BRAC Bank  
Biochemistry Olympiad, Department of Biochemistry and  
Molecular Biology, University of Dhaka.